International Journal of Greenhouse Gas Control 5 (2011) 1039–1054

Contents lists available at ScienceDirect

International Journal of Greenhouse Gas Control

journal homepage: www.elsevier.com/locate/ijggc

Monitoring of CO_2 storage in a depleted natural gas reservoir: Gas geochemistry from the CO2CRC Otway Project, Australia

Chris Boreham[a,b,*], Jim Underschultz[a,c], Linda Stalker[a,c], Dirk Kirste[a,d], Barry Freifeld[e], Charles Jenkins[a,f], Jonathan Ennis-King[a,g]

[a] CO2CRC, GPO Box 463, Canberra, ACT 2601, Australia
[b] Geoscience Australia, PO Box 378, Canberra, ACT 2601, Australia
[c] CSIRO Earth Science and Resource Engineering, PO Box 1130, Bentley, WA 6102, Australia
[d] Department of Earth Sciences, Simon Fraser University, Burnaby, BC V5A 1S6, Canada
[e] Lawrence Berkeley National Laboratory, One Cyclotron Rd, Berkeley, CA 94720, USA
[f] CSIRO Earth Science and Resource Engineering, GPO Box 664, Canberra, ACT 2601, Australia
[g] CSIRO Earth Science and Resource Engineering, Box 312, Clayton South, VIC 3169, Australia

ARTICLE INFO

Article history:
Received 19 May 2010
Received in revised form 21 March 2011
Accepted 27 March 2011
Available online 27 April 2011

Keywords:
Otway Basin
Carbon dioxide
Methane
Geosequestration
Depleted natural gas reservoir
Gas geochemistry
Carbon isotopes
Tracers
Waxy hydrocarbons
Monitoring

ABSTRACT

The CO2CRC Otway Project in southwestern Victoria, Australia has injected over 17 months 65,445 tonnes of a mixed CO_2–CH_4 fluid into the water leg of a depleted natural gas reservoir at a depth of ~2 km. Pressurized sub-surface fluids were collected from the Naylor-1 observation well using a tri-level U-tube sampling system located near the crest of the fault-bounded anticlinal trap, 300 m up-dip of the CRC-1 gas injection well. Relative to the pre-injection gas–water contact (GWC), only the shallowest U-tube initially accessed the residual methane gas cap. The pre-injection gas cap at Naylor-1 contains CO_2 at 1.5 mol% compared to 75.4 mol% for the injected gas from the Buttress-1 supply well and its CO_2 is depleted in ^{13}C by 4.5‰ VPDB compared to the injected supercritical CO_2. Additional assurance of the arrival of injected gas at the observation well is provided by the use of the added tracer compounds, CD_4, Kr and SF_6 in the injected gas stream. The initial breakthrough of the migrating dissolved CO_2 front occurs between 100 and 121 days after CO_2 injection began, as evidenced by positive responses of both the natural and artificial tracers at the middle U-tube, located an average 2.3 m below the pre-injection GWC. The major CO_2 increase to ~60 mol% and transition from sampling formation water with dissolved gas to sampling free gas occurred several weeks after the initial breakthrough. After another ~3 months the CO_2 content in the lowest U-tube, a further average 4.5 m deeper, increased to ~60 mol%, similarly accompanied by a transition to sampling predominantly gases. Around this time, the CO_2 content of the upper U-tube, located in the gas cap and an average 10.4 m above the pre-injection GWC, increased to ~20 mol%. Subsequently, the CO_2 content in the upper U-tube approaches 30 mol% while the lower two U-tubes show a gradual decrease in CO_2 to ~48 mol%, resulting from mixing of injected and indigenous fluids and partitioning between dissolved and free gas phases. Lessons learnt from the CO2CRC Otway Project have enabled us to better anticipate the challenges for rapid deployment of carbon storage in a commercial environment at much larger scales.

1. Introduction

Geological storage of CO_2 is a key component in the global effort on carbon capture and storage (CCS) to reduce greenhouse gas emissions. The two most volumetrically significant underground storage options are saline aquifers and hydrocarbon (gas and oil) fields; either depleted or as enhanced oil recovery (EOR) operations. Saline aquifers have potentially significant capacity of a size capable of storing all anthropogenic CO_2 emissions for many centuries (Hepple and Benson, 2003; Gunter et al., 2004), while hydrocarbon fields would only account for approximately half the CO_2 emissions projected to be released by 2050, assuming a 'business as usual' energy consumption model (Gale, 2004). Nevertheless, the greater geological and practical knowledge gained by the petroleum industry in hydrocarbon fields compared to saline aquifers make them attractive geosequestration sinks in the short to medium term. The CO2CRC Otway Project has targeted a depleted natural gas field for a large demonstration of geological storage of CO_2 and has relied on a wide range

* Corresponding author at: Geoscience Australia, PO Box 378, Canberra, ACT 2601, Australia. Tel.: +61 2 62499488.
E-mail address: chris.boreham@ga.gov.au (C. Boreham).

1750-5836/$ – see front matter.
doi:10.1016/j.ijggc.2011.03.011

of geological, geophysical and geochemical techniques in order to better understand the subsurface behaviour of supercritical CO_2.

1.1. CO_2 storage projects

Although world-wide there are many dozens of CCS projects planned only a handful are of commercial scale CO_2 storage projects. The Sleipner Project, the In Salah JIP and the International Energy Agency (IEA) Weyburn Project are to date the most significant commercial scale CO_2 storage projects. The offshore Sleipner project in the North Sea has injected over 1 Mt/y of CO_2 into a saline aquifer at ~1000 m sub-seafloor since 1996 (Zweigel et al., 2004). The In Salah project in Algeria commenced in August 2004 and by the end of 2008, over 2.5 million tonnes of CO_2 had been stored in a Carboniferous Age saline sandstone reservoir at 1900 m (Ringrose et al., 2009). The IEA Weyburn CO_2 Monitoring and Storage Project in a carbonate reservoir in onshore Canada commenced injecting 5 Kt/d of CO_2 in 2000 and will store 20 Mt of CO_2 over its lifetime (White et al., 2004) (http://www.ptrc.ca/siteimages/Summary_Report_2000_2004.pdf).

The Sleipner project relies solely on geophysical imaging of the developing CO_2 plume. The Weyburn project incorporates extensive well-based sampling, however, the Weyburn wells are optimised for enhanced oil recovery operations rather than primarily carbon storage. At In Salah, a wide range of monitoring techniques are being employed including collection of geological, geochemical and geophysical datasets enabling observation of breakthrough of CO_2 using a suspended appraisal well, 1.3 km away from the injection well, with the detection of fluorohydrocarbon tracers (Ringrose et al., 2009).

At the other end of the volumetric spectrum, small pilot projects involving Kt quantities of CO_2 were carried out at the Nagoaka Project (Mito et al., 2008) and the Frio Brine Pilot (Hovorka et al., 2006). The Nagaoka Project in Japan injected just over 10 Kt CO_2 into a saline aquifer at 1100 m. Geophysical well logging was used to detect CO_2 breakthrough at the monitoring wells while analysis of a time-series of samples collected using a cased hole dynamics tester helped resolve CO_2-fluid-rock reaction processes (Mito et al., 2008). In the Frio Brine project (Hovorka et al., 2008) ~1600 tonnes of CO_2 was injected into a sandstone saline aquifer at a depth of 1500 m (Freifeld et al., 2009) and employed intensive monitoring over a short timeframe with only 30 m between the injection and observation wells. The Frio Brine project also involved the extensive use of tracers and the deployment of the U-tube fluid sampler (Freifeld et al., 2005; Freifeld and Trautz, 2006), which enabled almost continuous downhole fluid collection, allowed real-time detection of the developing CO_2-rich plume and identification of the arrival (breakthrough) of the CO_2 at the observation well. Furthermore, the use of CO_2 with a distinctive carbon isotopic signature proved to be an effective tracer of the injected CO_2, both at Frio (Kharaka et al., 2006) and Weyburn (Shevalier et al., 2004; Raistrick et al., 2006).

Although the Sleipner and Weyburn projects are vanguards for the size required in the commercial geosequestration solution, they were not specifically setup to exclusively or inclusively monitor subsurface processes. On the other hand, the smaller pilot projects suffer from limitations in size and relevance in up-scaling. Therefore, to fill the significant 'size gap' in our knowledge, two large pilot scale projects involving significant CO_2 injection volumes and with an extensive monitoring and verification focus have recently commenced; the CO2CRC Otway Project in a depleted gas reservoir (Sharma et al., 2007, 2009) and the CO2SINK project in a saline aquifer at Ketzin, Germany (Schilling et al., 2009), both involving ~0.1 Mt CO_2 and making extensive use of remote monitoring and fluid sampling.

1.1.1. CO2CRC Otway Project

The CO2CRC Otway Project is the first demonstration of geological CO_2 storage in Australia and is the most monitored demonstration of CO_2 storage in a depleted natural gas field (Sharma et al., 2007, 2009). An ongoing study on CO_2 injection into a depleted gas field in the North Sea has its focus on enhanced gas recovery (EGC) and not intrinsically CO_2 storage (Vandeweijer et al., 2009). To meet scientific and regulatory requirements the CO2CRC Otway Project incorporates a wide-ranging monitoring and verification (M&V) program Underschultz et al., 2008). Geochemistry forms one component of the overall M&V strategy with the goals of: (1) establishing a robust protocol for the collection and analysis of representative subsurface samples; (2) validating our understanding of the geochemical processes affecting CO_2–methane–water–rock interaction; (3) developing guidelines for M&V operations for commercial geosequestration; and (4) meeting obligations to the Environmental Protection Agency and providing assurance to regulators and the public (Underschultz et al., 2008).

The CO2CRC Otway Project is located about 25 km northwest of Port Campbell, Victoria, Australia just inland from the coastal area known as the Great Ocean Road (Fig. 1). The CO_2-rich (average 75.4 mol% CO_2 and 20.5 mol% CH_4) Buttress-1 supply well was a suspended gas exploratory well, which remained unproduced. To utilize the Buttress-1 gas for the purposes of our storage demonstration, the gas is dried, compressed and piped 2.25 km to the nearby, newly drilled CRC-1 injection well. Injection of a CO_2–CH_4 mixed fluid began on 18th March 2008 and ceased 528 days later on 28th August 2009. A total of 65,445 tonnes of the CO_2-rich fluid was emplaced into the Waarre Formation Unit C (Waarre-C) at ~2 km depth. The suspended Naylor-1 production well was recompleted to serve as an observation well. The CRC-1 and Naylor-1 wells are 300 m apart within the same structural closure of the now partially depleted natural gas field (Fig. 2).

Baseline fluid samples were collected from Buttress-1, CRC-1 and Naylor-1 prior to injection commencing in CRC-1 on the 18th March 2008 (Boreham et al., 2008). Surface injection pressures are maintained at around 11 MPa (downhole pressure at the perforated interval is about 17.86 MPa at the start of injection, and rose to about 19.25 MPa by the end of injection) and fluid injection rates up to 160 tonnes/day (mean 124 tonnes/day). Such injection rates are comparable to acid–gas (H_2S–CO_2 mixtures) disposal into deep geological formations in Canada over the last two decades (Bachu and Gunter, 2004). The introduced plume is driven under injection pressure into the reservoir and subsequently moves also by buoyancy through the reservoir (16% average porosity and about 1Darcy average permeability) towards the Naylor-1 observation well. The migrating plume is expected to sweep up some of the estimated 20% residual methane saturation remaining in the water leg below 2039.5 mRT (Fig. 2; at Naylor-1 mRT 51.09 m + mSS).

The integrated M&V system installed at Naylor-1 consists of a number of purpose-built tools and facilities. These include three U-tube fluid samplers (Freifeld et al., 2005; Freifeld and Trautz, 2006), the associated field laboratory used to acquire the fluid samples at reservoir pressure and the slip-stream tracer injector system (Stalker et al., 2009). The latter was used to deliver three tracers, CD_4 (2000 L), Kr (20,000 L) and SF_6 (312 kg or approximately 50,000 L at 15 °C), which were co-injected with the CO_2–CH_4 fluid at CRC-1 over a 2-day period on the 4th and 5th April, 2008. The higher quantity of SF_6 was deemed necessary for the event of leakage to surface. Concentrations of >1 ppm, which upon dispersion would be detectable above background atmospheric concentrations at the atmospheric monitoring station (Etheridge et al., 2005; Leuning et al., 2008).

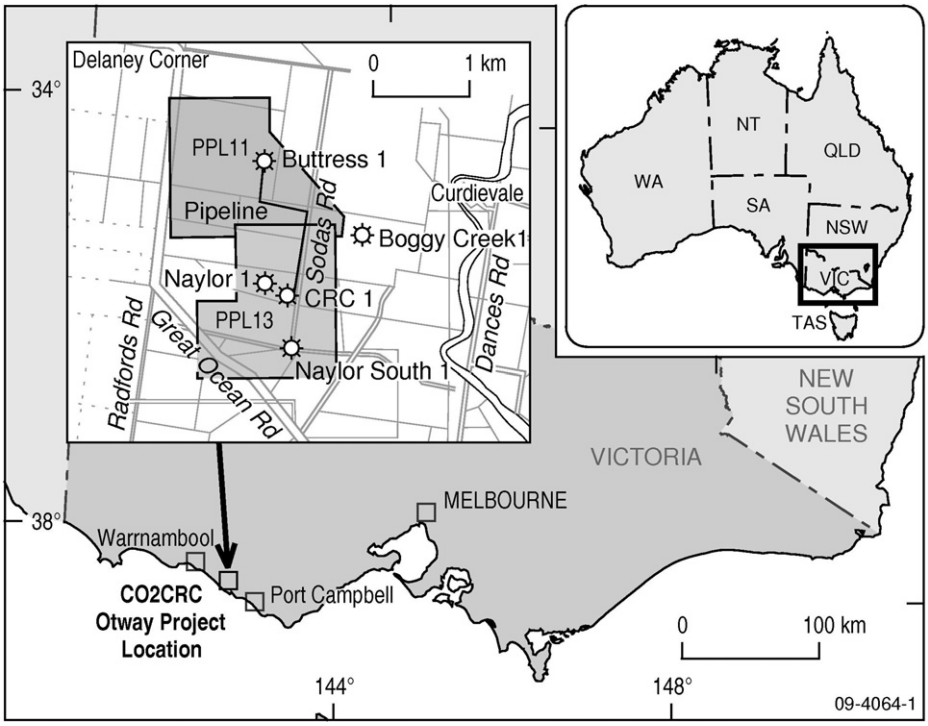

Fig. 1. Location map of the CO2CRC Otway Project.

The injected tracers were used to confirm breakthrough of injected CO_2 at reservoir level in the Naylor-1 well and as a part of other assurance monitoring objectives, including soil gas (Watson et al., 2006), atmospheric (Etheridge et al., 2005) and shallow ground water monitoring (Hennig et al., 2008; de Caritat et al., 2009). The tracers were introduced to the injection gas stream after the initial injection of 1000 tonnes of the CO_2–CH_4, which allowed for the establishment of a stable CO_2-rich gas plume around the wellbore prior to the introduction of the tracers (Stalker et al., 2009).

At the reservoir level, a combined geochemical and geophysics integrated bottom hole assembly (BHA) was installed. It consisted of three U-tubes (Freifeld et al., 2005; Freifeld and Trautz, 2006), two pressure/temperature sensors, numerous hydrophones and 1- and 3-component geophones (Fig. 2; Underschultz et al., 2008). The upper U-tube (U1) at 2028.8–2029.4 m drill depth from the rotary table (mRT) has access to the residual gas cap, while the two lower U-tubes (U2 and U3) are below the post-production gas–water contact (GWC) at 2039.5 mRT; U2 located at 2041.8–2042.4 mRT and U3 at 2046.3–2046.9 mRT. The U-tubes are isolated from the remainder of the wellbore using an inflatable packer set at 2022 mRT (Fig. 2).

The U-tube system provides access to the reservoir fluids for repeat sampling, with the fluids taken at the field laboratory experiencing minimal alteration by maintaining reservoir pressures until the samples are at surface and depressurization can be controlled. Geochemical analysis could help identify important rock–water–gas reactions. Sampled fluids would also be used to elucidate the transport pathways where several competing hypotheses were considered for the expected response. Knowing that the injected gas is considerably denser than the residual gas in the gas cap, it was unclear if the introduced gas would travel at the interface of the gas–water contact. Furthermore, it was anticipated that the continued injection of gas would lead to an eventual depression of the gas–water contact. Another possibility considered was stratigraphic control, in the form of shale baffles and the heterogeneous permeability structure, which would result in the CO_2-rich fluid arriving higher up in the gas cap and mix within the residual gas cap. The locations of the U-tube sampling inlets were chosen to help address those uncertainties.

This paper discusses the sub-surface gas geochemistry and includes results obtained pre- and post-injection. We discuss some of the operational challenges that were met and overcome and present some preliminary interpretation on the observations. The paper is part of a series focussing on various geochemical aspects e.g. tracers, inorganic geochemistry, soil and atmospheric gases, groundwaters and of the M&V operations at the CO2CRC Otway Project.

2. Sample collection and analysis

Gas samples were collected from the Naylor-1 well through a specifically designed triple U-tube sampling array, which was part of the bottomhole assembly (BHA) (Underschultz et al., 2008; Freifeld et al., 2009). Each of the three U-tubes consists of two 1/4″ stainless steel tubing lines (0.152″ id) connected by a tee with a check valve and a cylindrical 40 μm stainless steel inlet filter of 0.6 m length. The BHA was deployed from surface to ~2 km down the Naylor-1 well, giving each U-tube loop a volume of ~36 L. Formation fluid enters the well bore through perforations in the casing at 2028–2032 and 2039–2055 mRT, which extend to above and below the U-tube filter intakes. The U-tube sampling locations were selected so that any changes in the chemistry of the methane gas cap could be monitored, the initial breakthrough of CO_2 at Naylor-1 could be observed close to the GWC, and constraints on storage capacity and filling of the Naylor structure could be timed with eventual sampling of CO_2 from the lowermost U-tube.

The Naylor surface monitoring facility consists of a sample collection system for high pressure fluid and high and low pressure gas samples (Fig. 3). Upon opening the U-tube lines at the surface facility, the wellhead pressure rapidly drops and consequently formation pressure exceeds the pressure inside the U-tube, resulting in the check valve opening and formation fluid filling the U-tube.

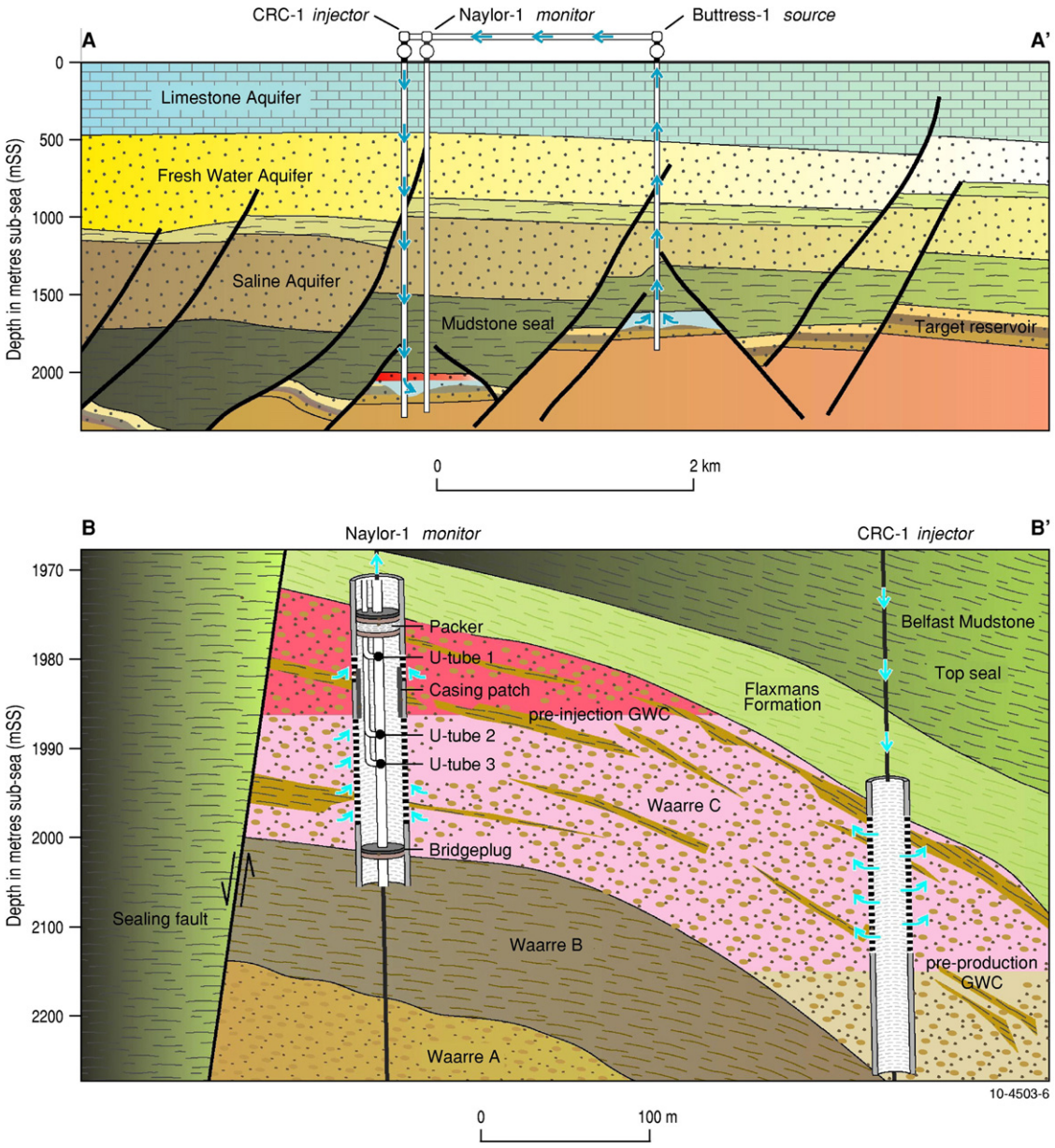

Fig. 2. Schematic cross-section of the Otway Project field site showing the relationship between the surface and subsurface installations, the Buttress-1 supply well, CRC-1 injection well and Naylor-1 observation well.

Gas was obtained directly from U1, as this has access to the residual methane gas cap, which self-lifts gas to surface at reservoir pressure (wellhead pressure of U1 is ~15.7 MPa). Gases are collected in both Swagelok SS cylinders (HP in Appendices 1 and 2; 150 ml capacity and rated to 34.5 MPa) and Isotubes™ (HP-I in Appendices 1 and 2; 110 ml capacity and rated to 690 kPa) connected in series. The SS cylinder was first filled to formation pressure, isolated then the gas pressure slowly released to flow gas through the Isotube. The procedure was repeated and the Isotube removed once the pressure had fallen to 345 kPa (this sample was considered as a field back-up sample). The SS cylinder was then re-pressurized to reservoir pressure and disconnect from the sampling line. This venting process resulted in variable cooling of the SS cylinder and Isotube and is a likely source of compositional fractionation that is evident when comparing the results between the HP and HP-I samples (Appendix 1). Following analyses back in the laboratory, an Isotube sub-sample of the high pressure gas in the SS cylinders was taken using a fill-purge cycle (repeated 5 times). The SS cylinder was then vented, washed with dichloromethane, evacuated and recycled back to the Otway Project site. Since different laboratories were used for different types of analyses, the same Isotube sample was not necessarily used for all the analyses. For example, the tracer results for the HP samples were generally from the Isotube sub-sample taken back in the laboratory.

The lower two U-tubes, positioned below the GWC, initially accessed the formation water, which did not flow to surface. Therefore, a N_2-assisted lift was required to push (N_2 down the Drive leg or upstream lines in Fig. 3) the formation water to surface for sampling. After the U-tube lines have been flushed with high pressure N_2 at 24.1 MPa, the N_2 pressure is released to atmosphere allowing fresh formation fluid to fill the U-tube through the opened down-hole check valve. High pressure nitrogen (24.1 MPa) is reintroduced to the upstream 1/4″ lines of the U-tube being sampled. This closes the downhole check valve and mobilises the fluid sample up the 1/4″ downstream line (sample leg in Fig. 3) to surface at formation pressure (~13.8 MPa). The fluid fills the 13 L SS sam-

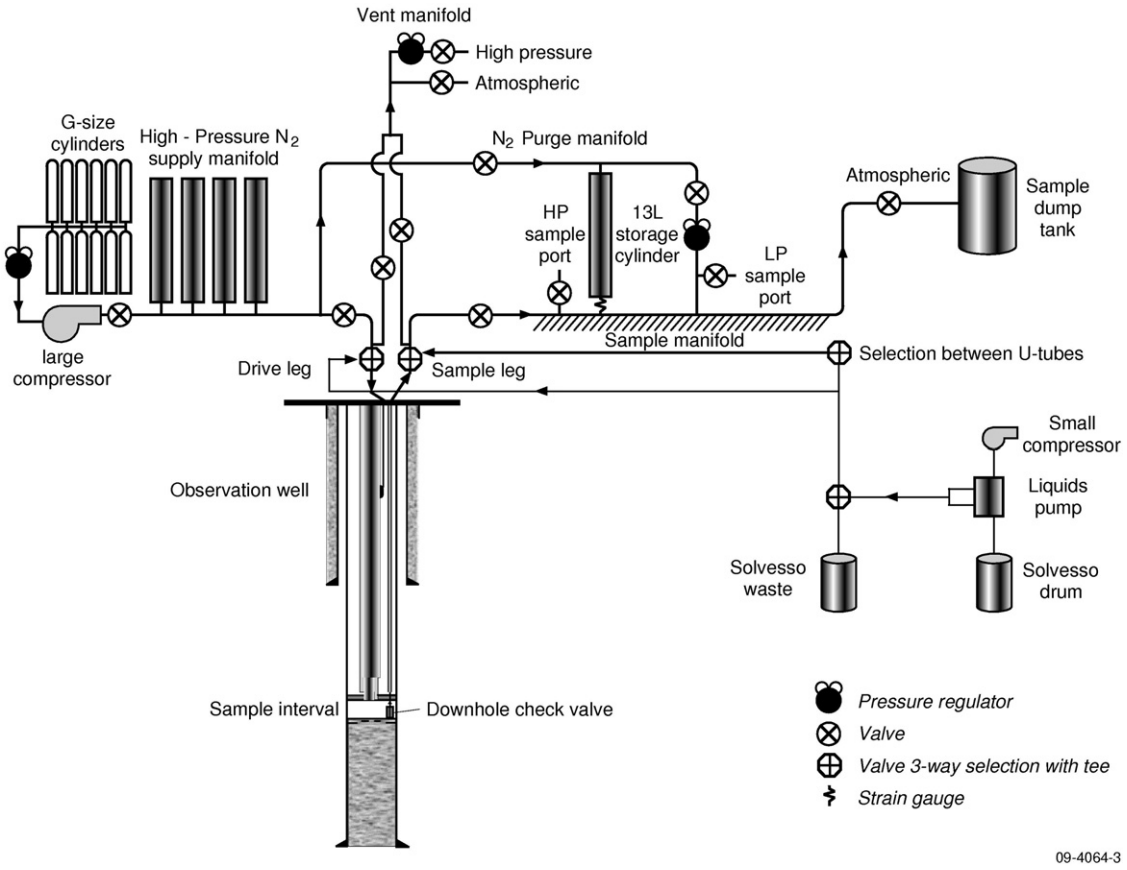

Fig. 3. Simplified schematic of the Naylor surface monitoring facility incorporating the U-tube sampling and the solvent delivery/retrieval systems. Note only a single U-tube is shown for simplicity.
Modified from Freifeld and Trautz (2006).

ple holding cylinder to formation pressure (Fig. 3). Sub-samples are then taken in two Swagelok SS cylinders connected in series (HP sample port in Fig. 3). This is a modification to the procedure reported by Freifeld et al. (2009), which employed further 'fill-and-dump' cycles, and in hindsight was an over-reaction to the management of the wax problem (see Section 2.2). Slowly releasing the pressure from the top of the 13 L sample holding cylinder allows the evolved solution gas to flow through a low pressure perspex water trap (1.3 L) and then through an Isotube (LP sample port in Fig. 3). When the pressure in the outside 13L container has dropped to 345 kPa a low pressure Isotube sample is taken (LP-I in Appendices 1 and 2). From one of the small SS cylinders, the valve is carefully opened and the formation water is allowed to fill a 27 ml glass vial (in triplicate). Once the effervescence had subsided, 3 ml of formation water is withdrawn from the full vial, which is then stoppered and crimp sealed with an aluminium lid to retain a headspace gas sample (H in Appendix 2).

Throughout the course of gas injection period, Buttress-1 gases were collected both before the separator at the Buttress production plant and at the CRC-1 injection well before the gases were deployed sub-surface (Appendices 3 and 4).

Molecular composition of the gas was determined using an Agilent 6890 gas chromatograph (GC) fitted with a series of 1/8″ packed columns and the GC oven held isothermal at 100 °C (Boreham and Edwards, 2008). The gas sample (Buttress-1, HP, HP-I, LP-I) was flowed at 30 ml/min for 1 min through two gas valves (0.5 ml and 2 ml sample loops) connected in series; the headspace gas sample (H) was manually injected using a gas tight syringe. Injection through the 0.5 ml loop in a helium carrier gas resulted in the analysis of the C_1–C_5, C_{6+}, O_2, N_2 and CO_2 with TCD detection. The mol% was determined against an external synthetic natural gas standard (mol%) with 62.95 C_1 or CH_4, 10.0 C_2, 10.1 C_3, 0.46 *i*-C_4, 2.99 *n*-C_4, 0.50 *i*-C_5, 0.51 *n*-C_5, 0.32 C_{6+}, 6.96 N_2, 5.21 CO_2 (Appendices 1 and 3). The experimental error for CO_2 (1× standard deviation) is ±2% of the reported value and the detection limit for CO_2 is 0.02 mol% (5× signal-to-noise). Samples with high air content (>10 mol%), due to leaking cylinders or ineffective flushing of Isotubes and those with elevated wet gas contents, due to condensate build-up, were excluded from further discussion.

Gas chromatography-combustion-isotope ratio mass spectrometry (GC-C-IRMS) was used to determine the carbon isotopic composition (all results reported in per mil VPDB) of CO_2, methane and ethane (Appendices 2 and 4) using the procedure of Boreham and Edwards (2008). The experimental error is ±0.3‰ (1× standard deviation).

Tracers were analysed by gas chromatography–mass spectrometry operated in a single ion recording mode (GCMS-SIR) using procedures described in Boreham et al. (2007) and Stalker et al. (2009). Briefly, CSIRO's Micromass AutoSpec-Q was used for GCMS-SIR analysis and operated at a resolution of 1000. A gas tight syringe was used to inject the gas sample (250 μl) into the heated (250 °C) split injector (25 ml/min split flow) and onto a fused silica 5 Å molecular sieve capillary column (50 m × 0.32 mm OD). Helium was used as carrier gas under a constant pressure of 25 psi. For SF_6 and CD_4 the column oven temperature was held isothermal at 40 °C where the tracers eluted in 2.3 and 13.3 min, respectively. For Kr the oven temperature was held isothermal at 200 °C and elution time was 4.4 min. CD_4, Kr and SF_6 were detected by monitoring masses 20.056, 83.912 and 126.964, respectively. He-only injections gave average (daily over 10 days of analyses) 'blank'

responses of 0.2 ppb, 30 ppb and 5 ppb for CD_4, Kr and SF_6, respectively. SF_6 was also detected at Geoscience Australia by GCMS-SIR (Agilent 5973) by monitoring mass-to-charge 127. A thick-film methylsilicone fused silica capillary column (BP-1, 50 m × 0.32 mm, 1 μm film thickness) was used under a constant flow of helium carrier flow of 2 ml/min. The column oven was held sub-ambient at −20 °C and under these conditions CD_4, SF_6 and Kr were partially separated with SF_6 eluting within 2 min. The analysis was performed in triplicate with repeated injections during a single data collection. A gravimetrically prepared gas mixture of 10 ppm (v/v) SF_6, Kr and CD_4 in helium was supplied by CoreGas (Sydney, Australia) and used (together with a 1:10 dilution of the gas standard in He) as an external standard to determine tracer concentrations in the gas samples. Reproducibility of the tracer concentrations was ±10% of the reported value. A more comprehensive description of the tracer methodology will be presented elsewhere.

2.1. Modelling of wellbore mixing effects

Due to the engineering complexity of installing a series of packers beneath the narrow diameter casing patch, multilevel sampling was performed in the slim Naylor-1 borehole without proper zonal isolation. This led to some uncertainty as to the source of the fluids being sampled given that the volumes extracted were comparable to the wellbore volumes. While the original gas production perforations near U1 were patched by the previous field operator, log evidence indicates that this patch was installed too deep, leaving at least a meter of open perforations. We took advantage of these open perforations by installing U1 at this depth to sample near the top of the gas cap. During the Naylor-1 recompletion effort, an additional length of casing, 2039–2055 mRT, was perforated to permit the lower two U-tubes to sample deeper in the reservoir, beneath the GWC. A series of U-tube extended flow tests, with the aim of investigating potential cross-contamination processes was undertaken over 2 days in December 2009. The time series geochemical data collected using a field quadrupole mass spectrometer (Freifeld and Trautz, 2006) substantiate that U1 fluids are distinct, both in composition and tracers, from U2 and U3. The same conclusion could not be made for the fluids collected from U2 and U3. We follow with the arguments to support these observations and our subsequent discussion of the U-tube data sets.

The BHA has some internal obstructions and fills most of the wellbore, but an annulus between the BHA and the casing is unobstructed. Since the sampling removes a volume comparable to the potentially mobile volume below the packer, significant mixing should be anticipated. However, the withdrawal rates are low (10–30 kg/h) and, given the high permeability of the adjacent formation, these rates are achieved with very small pressure differentials (a few kPa). We use a comparison of the pressure drawdown caused by flowing the U-tube during sampling, with the density contrast of the sampled fluids to investigate the potential for cross-contamination. The original gas in place (mostly methane) has a density of around 120 kg/m^3 compared to around 260 kg/m^3 for the arriving, CO_2-rich injected gas when diluted with native gas.

We can estimate the change in pressure required to draw the denser gases from U2 and U3 up to U1 by:

$$\Delta P_1 = (\rho_{U2} - \rho_{U1})gh \quad (1)$$

where g is acceleration due to gravity and h is the distance from U1 to the top of the perforated section of borehole near U2. Based on the length of unperforated casing between U1 and U2, h is 10 m and the density difference, $\rho_{U2} - \rho_{U1}$, between the U1 and U2 gas is 115 kg/m^3, we calculate the pressure drop that would lead to drawing U2 fluids up to U1 wellbore fluids to be 11.3 kPa. The driving force for drawing up fluids of different density would be the pressure decrease caused by production of the U-tubes. If we assume steady-state radial flow conditions to the well, which is a conservative assumption given that the early time pressure declines will be less during the transient period of flow, we can estimate the pressure decrease using Theim's equation as:

$$\Delta P_2 = \frac{Q\mu_0}{2\pi k k_r l} \ln\left(\frac{r}{r_w}\right) \quad (2)$$

We estimated the volumetric flow rate Q as being ~2.7×10^{-5} m^3/s during sampling by monitoring the rate at which pressure increased in the high pressure sample cylinders. Given a viscosity, μ_0 for the U1 fluid of 1.95×10^{-5} Pa s and assuming a flow thickness l as the estimated length of the perforated region at U1 of 1 m, formation permeability $k \times$ relative permeability k_r 2×10^{-12} m^2, and well radius, r_w is 0.035 m, and an assumption that the radius of infinite action, r, is 2 m, we calculate ΔP_2 to be ~0.17 kPa.

Since the decrease in pressure associated with flowing U1 is considerably less than the pressure required to raise the higher density fluid at the U2 level (0.17 kPa ≪ 11.3 kPa), we conclude that U1 cross-contamination with fluids at the U2 and U3 level is likely to be small. Similarly, when producing U2 or U3, the fluid at U1 is so much lighter than the fluid at U2 that fluid from U1 is not drawn down to the lower level.

U2 and U3 are placed closer together with an average 4.5 m depth difference. Given the volumes sampled, we expect fluid will mix between the two U-tube levels when both are producing water, and this is borne out by the similar water chemistry prior to self-lift (Kirste et al., 2009). Once U2 goes to self-lift, which happens abruptly over two weeks (see below), the U-tubes are sampling different fluids over a much more restricted catchment because the injected gas and formation water have very different densities. U2 samples an upper zone producing gas, whereas U3 samples a mixture of gas from this zone and water from a lower zone. In this case the density difference is 740 kg/m^3 and the implied ΔP_1 over h = 4.5 m is 32.6 kPa, so again we expect isolation of the two U-tubes during this phase.

Over a protracted transition to self-lift for U3, taking about six weeks, the water fraction declines and eventually self-lift ensues. Compositional measurements at U3 over this period reflect a varying combination of dissolved gas and free gas. Once both U2 and U3 are self-lifting, the wellbore between them contains mostly gas. With little density difference between the lower two U-tubes, we anticipate and later confirmed (see below) mixing will occur and indeed the compositions from this time on are very similar.

These considerations are idealized, but more detailed modelling suggests that the qualitative conclusions are robust. The density contrasts and production rates which are assumed in the above calculations are only typical values, however. For example, immediately after breakthrough at U2 the gas there is of low density and some communication with U1 may be expected, and indeed is observed.

2.2. Wax in gas

During injection, operational challenges were encountered that had the potential to derail the project. One of the most serious issues involved solid wax. At the surface in the Buttress-1 supply well, wax precipitation fouled production infrastructure and closed down the Buttress-1 plant. At Naylor-1, sub-surface build-up of wax in the U-tube 1/4″ SS lines prevented the delivery of U-tube fluids to surface, particularly in the upper U-tube sampling the gas cap.

The solid wax isolated from Buttress-1 was analysed by gas chromatography according to Boreham et al. (2008). The composition of the wax collected at Buttress-1 is dominated by a homologous series of n-alkanes that initially maximised at n-C_{27}. Samples taken more recently showed an increase of lower molecu-

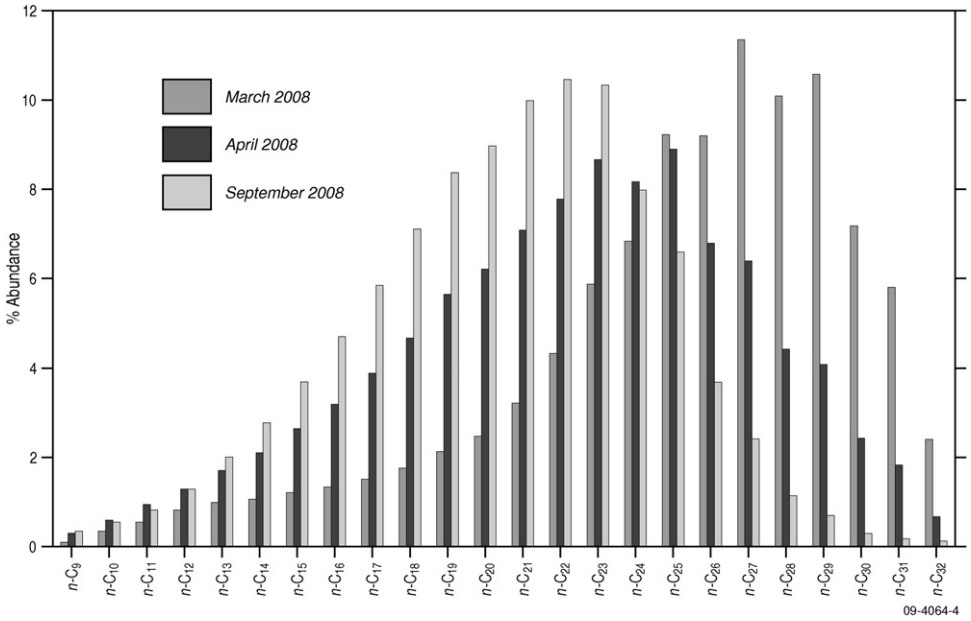

Fig. 4. Relative abundance of *n*-alkanes (from gas chromatography) in wax from Buttress-1 collected over time.

lar weight hydrocarbons with a maximum around *n*-C_{23}–C_{25} (Fig. 4) and a melting point of ~40 °C. At Buttress-1, precipitation of wax occurred in the production plant at the initial gas scrubber-flash pot. Here, the wellhead pressure during production was typically between 9.55 and 9.95 MPa but the temperature had fallen from a reservoir temperature of 85 °C to between 31 °C and 34 °C at the surface. This temperature drop allowed wax to separate from the gas. At Naylor-1, the temperature gradient was much more severe due to lack of continuous production, resulting in wax accumulation in the narrow 1/4″ U-tube lines in the subsurface. In fact, the U1 ceased flowing gas in early April 2008 as baseline sampling was being established and only after removal of a relatively small volume of gas from the Naylor-1 well. Wax precipitation during natural gas processing was also a problem for a dry gas field in Iran where solid wax formed at 32.6 °C at atmospheric pressure (Jeirani et al., 2007), although the higher relative wet gas contents of the Otway Project gases would support a higher wax load.

At Buttress-1, installation of heat tape to maintain the scrubber line at 48 °C has provided an adequate level of preventative maintenance, resulting in less fouling of the downstream flash pot. Nevertheless, daily venting of the lines (yielding about 40 L of white 'foam') together with periodic dismantling of scrubber lines and mechanical clearing of the internal wax residue is still required. The gas processing at the Buttress surface facility had the effect of slightly decreasing the wet gas (higher CH_4/C_2–C_5) and liquid hydrocarbon (higher C_2–C_5/C_{6+}) contents of the gas arriving at CRC-1 compared to the unprocessed gas from the Buttress-1 well (Appendix 3). On the other hand, the carbon isotopes of the gaseous C_1–C_5 hydrocarbons and CO_2 remain unaltered (Appendix 4). Interestingly, the relative amount of feedstock liquid hydrocarbons (including wax) from Buttress-1 showed an increase during the middle of the injection period during the hotter months from November 2008 to May 2009.

At Naylor-1, a solvent delivery and retrieval system (using a piston pump capable of 34.5 MPa outlet pressure) permitted Solvesso-100™ industrial solvent (ExxonMobil, Houston, TX, USA) to be pumped into either the drive or sample legs (Fig. 3). Generally, it was found that if only a limited volume (10 L) of solvent was introduced into the sample leg's 1/4″ SS tubing and allowed to soak for a period there is sufficient reservoir pressure to self-lift the solvent back out of the line and into a waste drum. After all the U-tubes began to access only gas, preventative maintenance required Solvesso-100 to be introduced into the U-tubes on a monthly basis. It is important that all solvent is removed from the U-tube line before sampling formation gases. Since the solvent has a higher density than the formation gas, the presence of Solvesso-100 in the U-tube lines could be identified by a reduction in the surface pressure of that line using wellhead-mounted pressure gauges. Both lines were allowed to flow gas until the pressures on the two lines equilibrated. This was an indication that all the solvent was removed from the lines and that no blockages remained.

3. Results

The analytical results of the baseline (pre-injection) and post-injection composition of the free and dissolved gases collected at the Naylor-1 observation well are listed in Appendices 1 and 2.

Commissioning of the Buttress-1 compression plant and intermittent injection of supercritical mixed gas into the CRC-1 well started on 18th March 2008 and continuous injection was transitioned to on 1st April, 2008. In the following discussion of Otway Project results "days after injection" refers to the time relative to commencement of injection on the 18th March 2008. Breakthrough is defined here as the first occurrence of measurable changes in the molecular and carbon isotopic composition of the U-tube gases, concomitant with the detection of added tracers, especially SF_6 and CD_4 which are both absent in the background sub-surface fluids.

3.1. Breakthrough of CO_2-rich gas

The arrival (i.e. breakthrough) of the migrating CO_2–CH_4 fluid at the BHA in Naylor-1 was confirmed by changes in the molecular composition of U-tube gases (Figs. 5 and 6) and the carbon isotopic composition of CO_2 (Fig. 7). A baseline and pre-injection study (Boreham et al., 2008) identified CO_2 as a natural tracer due to the low CO_2 content and ^{13}C-depleted CO_2 pre-existing in the Naylor-1 gas compared to the CO_2 in the Buttress-1 supply gas. Mass balance calculations suggest that ~1000 tonnes of 'Buttress' CO_2 was needed to mix with the residual gas cap at Naylor-1 to provide a measurable change in gas compositions (Boreham et al.,

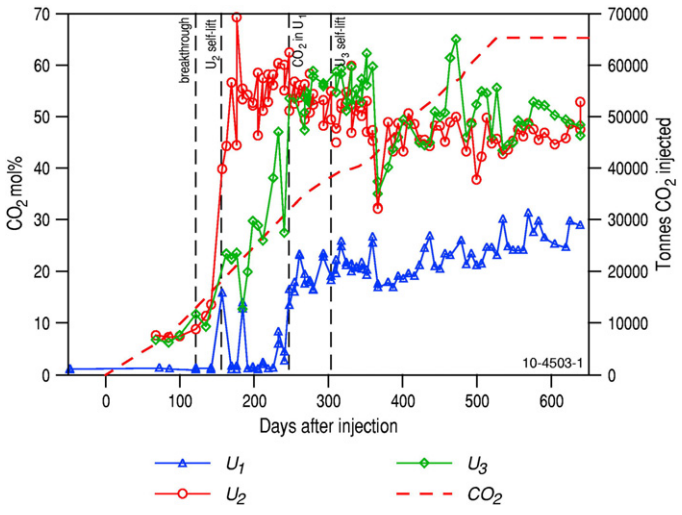

Fig. 5. Time series of U-tubes 1, 2 and 3 showing CO_2 content (mol% as N_2-free basis) of samples collected at Naylor-1 well, and cumulative tonnes of mixed supercritical CO_2–CH_4 injected into the CRC-1 well. *Note*: gases are from a high pressure (HP) sample collected either in a high pressure SS cylinder or a low pressure isotube, or a low pressure gas (LP) from depressurizing formation water to 345 kPa and the released gas collected in an isotube (see Appendix 1).

2008). On the other hand, the carbon isotopic composition of the methane and ethane collected at Naylor-1 cannot be used as a natural tracer since their $\delta^{13}C$ values are indistinguishable amongst the Buttress-1, CRC-1 and Naylor-1 gases and therefore do not change with gas mixing (Fig. 8).

3.2. Molecular composition

Breakthrough of the CO_2-rich fluid occurred at U2 between 100 (27th June 2008) and 121 (17th July 2008) days after injection (Fig. 5) with a measurable increase in CO_2 content above a baseline of 7.5 mol% CO_2 (N_2-free) at day 121 for the exsolved gas from formation waters (Fig. 5). This timing corresponds to 10,000–12,700 tonnes of CO_2 having been emplaced in the Naylor gas field via the CRC-1 injection well (Fig. 5). After this time, U2 displays a consistent rise in CO_2 mol% with an abrupt increase in CO_2 mol% between 142 (7th August) 2008) and 156 (21st August 2008) days. By day 177 (11th September 2008), U2 transition from N_2-assisted lift of formation water to a self-lifting gas to surface was complete after the injection of 21,100 tonnes of CO_2-rich fluid. The transition to self-lifting in U2 corresponds to the downward movement of the GWC to within the vicinity of the U2 inlet; a movement of at least 2.3 m (to top of U2 inlet filter) over the pre-injection GWC level. From mid-September 2008 to mid-February 2009 (~340 days), CO_2 contents in the free gas have consistently remained between 52 and 59 mol% in U2, well below the Buttress-1 supply gas, which varies slightly over the course of injection from 72 to 78 mol% CO_2 (average 75.4 mol%; $n = 7$; Appendix 3 'after separator'), 3–6% C_2–C_5 wet gases and 2–3% N_2 with the balance being methane. After mid-February, U2 showed a gradual decrease in CO_2 mol% to around 47 mol% over the last 2 months reported.

Over the above time period the CO_2/CH_4 ratio for U2 was initially very low (0.08) rising rapidly to an average of ~1.4 where it remained fairly constant for the remainder of 2008 after which time there was a steady decrease to its current value in mid-December 2009 of around 1.0 (Fig. 6b and Appendix 1). This compares to a CO_2/CH_4 ratio of 3.5 (±0.3, $n = 10$) for the injected gas at CRC-1. A similar time-series profile is seen for CO_2/ethane and CO_2/propane ratios from a pre-breakthrough ratio to a maximum ratio of 2.8–31 and 13–86, respectively (Fig. 6b, Appendix 1). The injected gas at CRC-1 has CO_2/ethane and CO_2/propane ratios of 93 ($\sigma = 9$, $n = 10$)

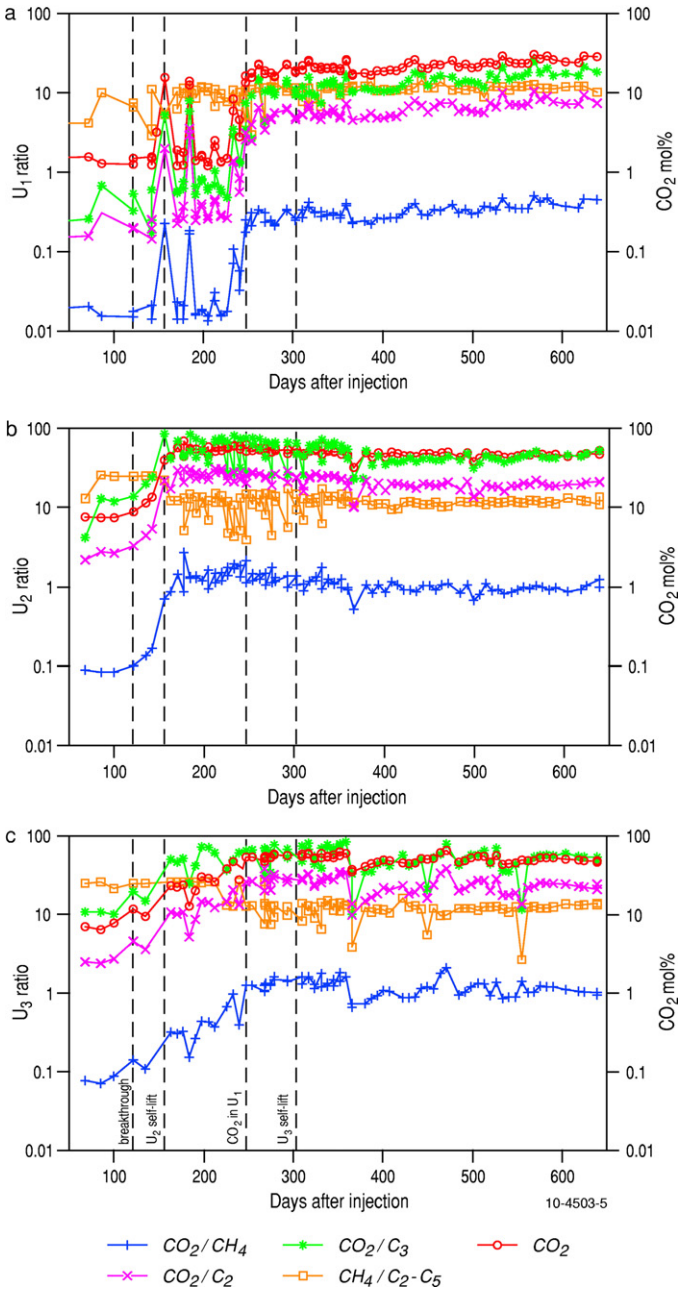

Fig. 6. Time series of ratios CO_2/CH_4, CO_2/ethane (C_2), CO_2/propane (C_3), CH_4/wet gases (C_2–C_5) and CO_2 mol% for (a) U-tube 1, (b) U-tube 2 and (c) U-tube 3. Note the log scale on primary and secondary *Y*-axes.

and 269 ($\sigma = 26$, $n = 10$), respectively. For U2, the pre-transition nitrogen to methane ratio (N_2/CH_4; Appendix 1) averages 0.84 (between 29th May 2008 and 7th August 2008) for the low pressure exsolved gas, reflecting the addition of external N_2 as part of the sampling procedure. After self-lift the ratio is 0.05 (average from 11th September 2008 to 19th February 2009) indicative of the low abundance of N_2 in the residual and injected gas. Differences are also seen in the proportion of hydrocarbon gas components. In U2, the exsolved gas has a lower wet gas content with C_1/C_2–C_5 ratio around 25 whereas after gas lift the free gas is much wetter after day 163 with a CH_4/C_2–C_5 ratio averaging around 12 (Fig. 6b, Appendix 1). The higher former ratio is a consequence of the preferential dissolution of methane compared to wet gases in the aqueous phase.

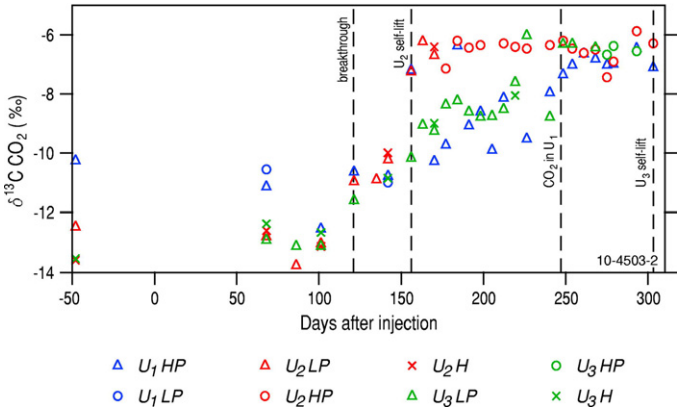

Fig. 7. Time series of U-tubes 1, 2 and 3 showing the carbon isotopic composition ($\delta^{13}C$ ‰) of CO_2. *Note*: HP = high pressure gas sample collected either in a high pressure SS cylinder or a low pressure isotube; LP = low pressure gas from depressurizing formation water to 345 kPa and the released gas collected in an isotube; and (c) H = headspace gas after transfer of formation water to a glass vial at atmospheric pressure.

U3 showed a sharp increase in CO_2 content to between 22 and 30 mol% as early as day 163 (28th August, 2008) at the same time as U2 became self-lifting and remained within this CO_2 range up to day 212 (16 October, 2008) (Fig. 5). No exsolved gas sample was taken on day 157 for U3 (beginning of self-lift at U2) since sampling targeted formation water at this time. The weight increase from the strain gauge readings for U3 indicated a dominant gas phase in the outside holding cylinder, consistent with pronounced wellbore mixing. U3 started transitioning to self-lifting gas in late October–mid November 2008 (days 226–247), signified by a jump from around 25 mol% to ~50 mol% CO_2 and following the cumulative injection of ~30,000 tonnes of mixed CO_2-rich fluid (Fig. 5). Nevertheless, it was only from day 310 (22nd January 2009) did the N_2/CH_4 ratio remain consistently low, indicating that U3 had fully maintained self-lift. During this intervening 'transition' interval between days 233 and 310 the main fluid collected at surface oscillated between formation water and gas. This was also confirmed by the variable weight of the filling fluid in the outside 13 L holding cylinder with values between pure liquid and pure gas (the weight increase on day 303 indicated only gas was collected in

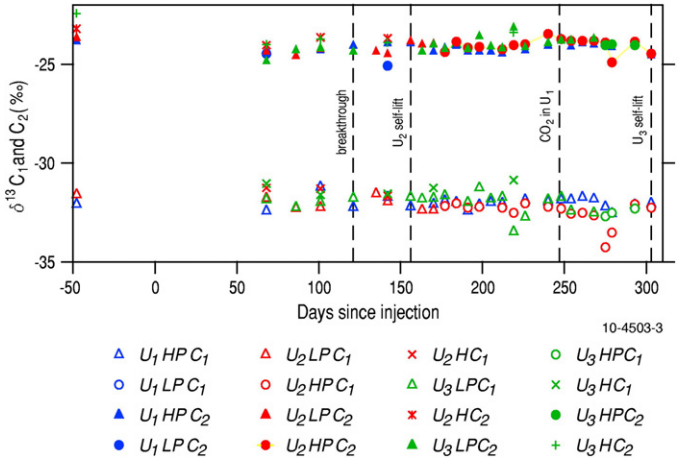

Fig. 8. Time series of U-tubes 1, 2 and 3 showing the carbon isotopic composition ($\delta^{13}C$ ‰) of methane and ethane. *Note*: HP = high pressure gas sample collected either in a high pressure SS cylinder or a low pressure isotube; LP = low pressure gas from depressurizing formation water to 345 kPa and the released gas collected in an isotube; and H = headspace gas after transfer of formation water to a glass vial at atmospheric pressure.

the holding cylinder). Given the potential for cross-contamination between U2 and U3, it is clear that the increases in CO_2 mol% are strongly influenced by wellbore mixing from the time of breakthrough at U2. The effects of wellbore mixing are also expressed by more gradual increases (compared to U2) in CO_2/CH_4, CO_2/ethane and CO_2/propane ratios up to self-lifting gas as a consequence of mixing with free and exsolved gas (Fig. 6c). Nevertheless, the wet gas content remained fairly constant up until day 212 (before onset of the transition to fully self-lifting) with an average CH_4/C_2–C_5 ratio of 25 (Fig. 6c, Appendix 1), indicating that the exsolved gas from formation water at U3 level is still a major contributor to gases collected up until the start of self-lifting gas after which the CH_4/C_2–C_5 ratio decreases by approximately a half.

By comparison, the always self-lifting U1 gas did not indicate the arrival of injected gas until day 247 (20 November, 2008) with a consistent increase up to approximately 20 mol% CO_2 on day 261 followed by a gradual rise to its present value after 639 days of approximately 30 mol% CO_2 (Fig. 5 and Appendix 1). The time of the initial rise in CO_2 content at U1 in late November 2008 slightly post-dates the final rapid rise in CO_2 content in U3. A similar overall trend is seen in the CO_2/CH_4, CO_2/ethane and CO_2/propane ratios at U1, resulting from the mixing of low-CO_2 Naylor-1 gas with the CO_2-rich injected gas (Fig. 6a). Before mixing (up to day 226) CO_2/CH_4, CO_2/ethane and CO_2/propane ratios averaged were 0.02, 0.39 and 0.82, respectively. After the arrival of the CO_2-rich gas and the mixed gas has stabilised at $CO_2 > 20$ mol%, the ratios are 0.29, 5.5 and 11.9 (average of days 261–450) and 0.38, 7.4 and 16.7 (average of days 457–639), respectively. The pre-injection Naylor-1 gas is slightly wetter (CH_4/C_2–$C_5 = 8.6$; Appendix 1 HP-only average) compared to the mixed gas signal after the arrival of the CO_2-rich gas (CH_4/C_2–$C_5 = 10.5$ for HP-only average of days 261–450 and CH_4/C_2–$C_5 = 11.6$ for HP-only average of days 457–639; Fig. 6a and Appendix 1). All U1 gases are much wetter than the injected gas at CRC-1 (CH_4/C_2–$C_5 = 16.9$; Appendix 3). Significantly, there are three early but transient rises in CO_2 mol% in U1 on days 157, 184 and 233 and all are attributed to transient wellbore mixing.

Although the compositional analysis of HP and HP-I samples are in general agreement there are some exceptions, particularly for gases with high CO_2 contents (U2 in Fig. 6b between days 177 and 331 where complementary HP and HP-I samples were measured). Here, the relative proportions of CH_4 and wet gases (Fig. 6 and Appendix 1) are dependent on the sampling procedure. The procedure of continuous flowing of gas through the Isotube results in molecular fractionation with a bias towards a lower relative abundance of CO_2 and higher wet gas content.

3.3. Carbon isotopic composition of CO_2

The carbon isotopic composition of CO_2 forms a natural tracer with U1 $\delta^{13}C$ CO_2 at −11.0‰ (average from 30/01/2008 to 7/08/2008) for the free gas. This compares with −13.0‰ (average from 30/01/2008 to 27/06/2008) for the CO_2 gas released from both U2 and U3 samples during depressurization of the formation water from reservoir pressure to 345 kPa (Fig. 7 and Appendix 2). Isotopic equilibrium between the dissolved and gas phase CO_2 at 20 °C (surface facility separation temperature) is calculated to be −1.1‰ (Vogel et al., 1970), suggesting that further depletion in ^{13}C for the initial exsolved CO_2 from U2 and U3 compared to U1 free CO_2 is likely to involve some other process like a kinetic Rayleigh-type distillation or mixing. No further significant carbon isotopic fractionation is seen for the headspace gas (H; Fig. 7 and Appendix 2), which represents an essentially degassed sample and shows a much higher CO_2 mol% (data not shown).

For U2, there is an abrupt increase in $\delta^{13}C$ of around 2‰ on day 121 (17th July 2008) in Fig. 7, coincident with the initial rise

in mol% CO_2 (Fig. 5). A larger enrichment in ^{13}C is observed concomitant with the major change in CO_2 concentration between days 142 (7th August 2008) and 156 (21st August 2008) and the transition from N_2-assisted gas lift of formation water to self-lifting gas is complete by day 177. Here, the carbon isotopic signal of the allochthonous CO_2 completely overwhelms the indigenous CO_2. After this time and up until the final isotopic measurement (day 303 on 15th January 2009), the CO_2 carbon isotopic composition has remained constant with an average of −6.5‰ (σ = 0.4‰, n = 13); the same isotopic value as that found in Buttress-1 supply gas (Boreham et al., 2008) (Appendix 4, average −6.7‰). The $\delta^{13}C$ CO_2 from U3 also shows the enrichment in ^{13}C on day 121 (17th July 2008) concomitant with the changes at U2, suggesting limited wellbore access to gas for the deeper U3 level at the time of breakthrough at U2. In comparison, the change in $\delta^{13}C$ CO_2 for U1 remains relatively small throughout the time that U2 and U3 have taken to stabilise at the $\delta^{13}C$ value of the injected CO_2. However, there is a trend towards enrichment in ^{13}C before the major increase in CO_2 mol%, indicating very minor access to CO_2-rich fluid from below. Wellbore mixing at U1 is confirmed with the two transient spikes in CO_2 content in U1 at days 156 and 184 (Fig. 5; day 233 was not measured for carbon isotopes) and accompanied by the expected enrichment in ^{13}C (Fig. 7). A consistent increase in $\delta^{13}C$ of CO_2 in U1 only occurs with the increase in CO_2 mol% in early November (Fig. 7; Appendix 2) and rapidly stabilises within a couple more weeks at the same isotopic value as the injected CO_2.

3.4. Tracers

The first detection of all three tracers above background levels (background concentrations of Kr are 0.3 ppm at the Buttress-1 and 0.17 ppm at Naylor-1; average of U1 values before breakthrough while SF_6 and CD_4 are below instrument blanks of around 1 ppb) occurs 121 days after injection, signifying the breakthrough of a dissolved phase of CO_2-rich fluid with the concentrations for SF_6, Kr and CD_4 at 0.019, 1.57 and 0.009 ppm, respectively (Fig. 9). The high abundance of Kr is due, in part, to its greater water solubility compared to the other two tracers. Tracers are also simultaneously detected at low levels at the upper and lower U-tubes as a result of limited wellbore mixing at this time. By day 170, with self-lift at U2 now established, there is a large increase in tracers concentrations at U2 with increases between 2 and 260 fold for SF_6, Kr and CD_4 to 4.9 ppm, 3.9 ppm and 0.18 ppm, respectively, together with large increases in U2/U1 and U2/U3 tracer ratios. Although the Kr concentration in the free gas from U2 only increased approximately 2-fold over that in the exsolved gas, there is an enormous difference in the absolute amounts of the gases (i.e. in the outside holding cylinder at 13.8 MPa: 13 L of formation water with minor relative amounts of dissolved gas before self-lift compared to 13 L of pure free gas after self-lift). Such large concentration differences between the U-tubes signifies that each generally accesses formation fluids at their respective levels, especially at times of maximum density contrasts between the three U-tubes. Generally, peak tracer concentrations for SF_6 and Kr occurred around the beginning of the transition to self-lift in U2 and U3 and the arrival of the CO_2-rich fluid at U1 (Fig. 9). This is expected because the injected CO_2 preferentially dissolves in the water phase, concentrating the gas phase tracers at the head of the injection plume. On the other hand, CD_4 concentrations maximise much later and remain fairly constant thereafter, especially for U1 (Fig. 9). Given the large amount of CH_4 residually trapped and dissolved, the injected CD_4 will likely undergo significant exchange with the native CH_4, retarding its rate of transport in comparison to SF_6 and Kr. The transient increase in tracer concentrations at day 156 in

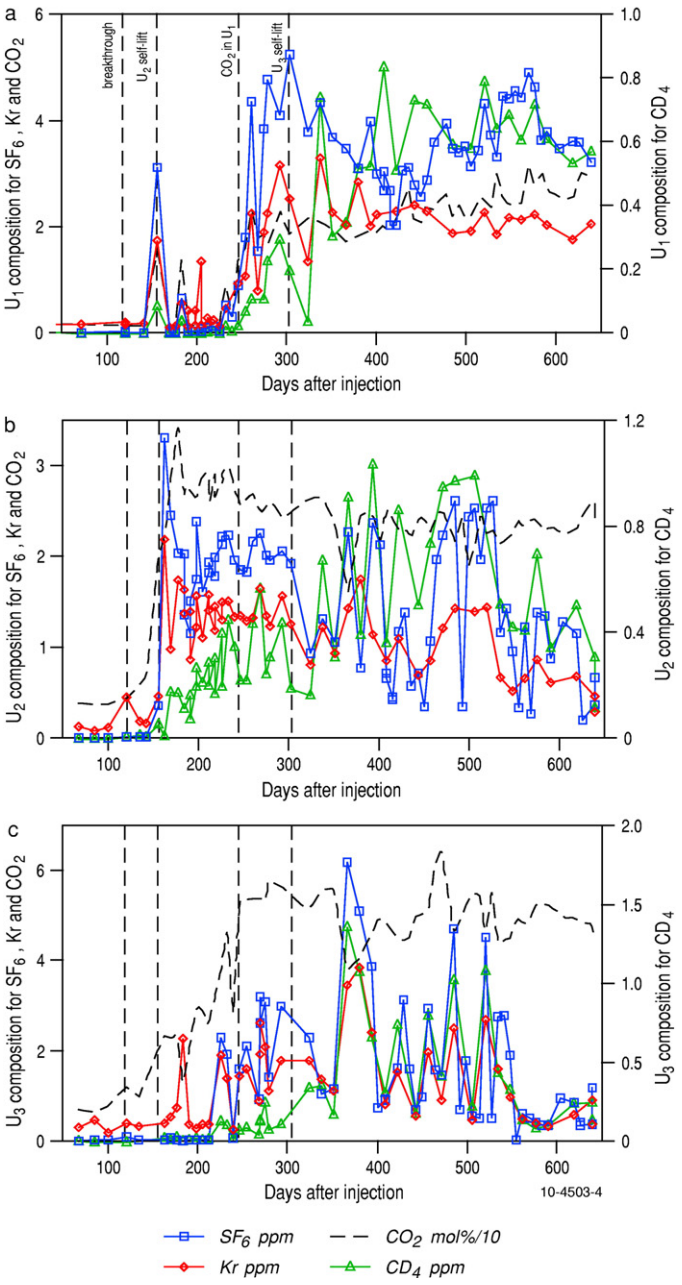

Fig. 9. Time series of SF_6 and Kr (primary *Y*-axis) and CD_4 (secondary *Y*-axis) tracer concentrations (ppm) for (a) U-tube 1, (b) U-tube 2 and (c) U-tube 3. Note CO_2 mol% is divided by 10 (primary *Y*-axis).

U1 coincide with a similar rise in CO_2 mol% (Fig. 5) and increase in $\delta^{13}C$ CO_2 (Fig. 7) and is again attributed to significant wellbore mixing. By day 639, tracer concentrations have generally fallen at U2 and U3 but have maintained consistently high values for U1 (Fig. 9).

4. Discussion

4.1. Measures of wellbore mixing

Access limitations within the Naylor-1 wellbore at the reservoir level dictated that the BHA was deployed with only a single packer. This was placed above the upper U-tube and served to isolate the U-tubes from the overlying wellbore. With such a configuration, complications involving wellbore mixing need to be accounted for

and deconvoluted from localised fluids entering through the perforations at the level of the individual U-tube inlets. Flow modelling (see Section 2.1 above) indicates that fluid flow into the wellbore is controlled primarily by deliverability (i.e. permeability of the rock matrix) and fluid composition; the denser fluids cannot readily overcome the gravitational force and rise to higher levels. Density contrasts, from highest to lowest, are CH_4-rich gas–water, CO_2-rich gas–water, CH_4-rich gas–CO_2-rich gas and water–water. The composition of the collected fluids generally conforms to these partitions.

Before day 121 and breakthrough, the fluids are CH_4-rich gas–water (U1–U2 and U1–U3) and water–water (U2–U3). The respective compositions from the U-tubes show no mixing between U1 and the lower U-tubes whereas formation waters collected from U2 and U3 are geochemically similar possibly but not conclusively as a result of maximum wellbore mixing. During the transition of U2 from N_2-assisted lift of formation water to self-lifting CO_2-rich gas, there is a maximum disturbance in the density and flow contrast between all three U-tubes and the compositional changes in the collected fluids reflect this. At initial breakthrough, it is difficult to explain the first detection of all tracers at all U-tube levels without the involvement of wellbore mixing. Subsequent samples confirm that this early detection of tracers at U1 and U3 was most probably spurious. Wellbore mixing at U1 is generally considered very minimal and below the resolution provided by molecular composition (Figs. 5 and 6) and carbon isotopes of CO_2 (Fig. 8). Nevertheless, transient spikes in composition at U1 of all measured parameters (molecular composition, carbon isotopes and tracers) are seen in gases collected on days 156 and 184. The former is coincident with the arrival of the main phase of CO_2-rich gas at U2 and is likely to represent wellbore mixing at a time of rapid change in CO_2 gradients and flow dynamics within the vicinity of the wellbore. The reason for the second transient rise (day 184) is unclear, though coincident with a rise in CO_2 mol% at U2 but a fall in the CO_2 content at U3. Factors external to the wellbore (e.g. deliverability and formation heterogeneity) may also be involved as the GWC moves down. The transient increase in CO_2 mol% and tracer concentrations on day 233 is attributed to wellbore mixing in response to the onset of transitioning to self-lifting at U3.

The extent of wellbore mixing between U2 and U3 remains variable even after U2 is producing CO_2-rich gas and U3 producing water. The modelled 'catchment' for the fluid entering U-tube is within ± 2 m of the level of the U-tube filter. The close proximity between the two lower U-tubes (3.9 m separation between to top of the inlet filter at U3 and the base of the inlet filter at U2) would indicate some overlap in accessed fluids outside the wellbore. The strain gauge readings on U3 enabled resolution of the fluid composition from day 226 (8th November 2008) with variable relative proportion of water and gas. Before this time, fluids were dominated by formation water and the wet gas contents confirm a bias towards dissolved gas. The time of the initial rise in U1 in early November 2008 is similar to the time U3 started transitioning to gas lift and there is the possibility that both events could be interconnected. The response of the tracer data (Fig. 9 and Appendix 1) and CO_2 content show an initial increase at U1 on day 233. Significantly, the CO_2 content of U1 is still lower than the two deeper U-tubes.

Continuous flow tests from the three U-tubes were performed in December 2009 and immediately before the last reported results. They confirmed that U1 composition and tracer content are distinct from that at the lower U-tubes. Therefore, over the course of the study the compositional behaviour at U1 generally remains independent from U2 and U3, attesting to the limited wellbore mixing between the uppermost and lower U-tubes, especially once all are producing gas and above the GWC.

Table 1
Mole fraction dissolved gas components.

Compound	Model	Measured
CO_2	0.12	0.075
CH_4	0.84	0.89
C_2	0.026	0.028
C_3	0.0085	0.0062
i-C_4	0.0071	0.00065
n-C_4	0.0011	0.009
i-C_5	0.00015	0.0002
n-C_5	0.00017	0.00019
C_{6+}	0.00036	0.00046

Model = calc. from free gas U1 day 170.
Measured = dissolved gas at for U2 day 100.

4.2. Observed versus modelled gas molecular and isotopic compositions: U-tube performance

In U-tube 1, the pre-injection high pressure sample free gas averages 1.5 mol% CO_2 ($\sigma \pm 0.3$ mol%, $n = 26$, air and N_2-free basis to day 226; Appendix 1), while the low pressure sample gases, representing the dissolved gas below the GWC, from U-tube 2 average 7.5 mol% CO_2 ($\sigma \pm 0.1$ mol%, $n = 3$, air and N_2-free basis to day 100; Appendix 1) before self-lift. This difference reflects the preferential solubility of CO_2 in the aqueous phase relative to the other gases present.

The observed free to dissolved gas relationship can be compared with modelled compositions and used to ascertain the performance of the U-tube sampling methodology. Henry's law constants were calculated for each of the gas phase species at pressure and temperature using methods of Krause and Benson (1989), Trew et al. (2001), Fernandez-Prini et al. (2003) and Majer et al. (2008). While the semi-empirical correlation of Trew et al. (2001) accounts explicitly for non-ideality of SF_6, fugacity coefficients for the CO_2 and C_1–C_6 hydrocarbons were calculated using a Peng and Robinson (1976, 1980) equation of state for gas mixtures using binary interaction parameters (Reid et al., 1977; Jaubert and Mutelet, 2004; Vitu et al., 2008). The effect of salinity on the solubility of the dissolved gas species was determined for the hydrocarbons using the method of Søreide and Whitson (1992) and for CO_2, that of Helgeson (1969).

Each modelled dissolved gas component's content in equilibrium with the U1 day 170 gas is shown in Table 1 along with the N_2-free data of U2 day 100. In general, the model results match the measured values fairly well except for CO_2 which shows the largest variance and is outside experimental error. The relatively high solubility of CO_2, even at the lower P and T of sampling, means that a greater proportion of CO_2 stays in the aqueous phase and thus the exsolved concentration is less than the modelled. Evidence that this is contributing to the discrepancy lies in the composition of the headspace gas (H), which typically gave much higher CO_2 contents than the corresponding exsolved (I) samples. Another factor contributing to the low CO_2 exsolved may be CO_2–water–rock interaction in the aqueous phase. Geochemical modelling indicates that the system is at equilibrium between the dissolved CO_2 and the dominant carbonate mineral phase present and the modelled CO_2 fugacity is consistent with the measured exsolved content rather than the gas phase value (Kirste et al., 2009). This implies that the rate of diffusion of CO_2 from the gas phase into the water leg is less than the reaction rate and the measured exsolved CO_2 content is less than predicted in Table 1 because of pH buffering and carbonate precipitation.

The relative success of the predictive model enabled the generation of a mixing model to evaluate the evolution of the aqueous phase gas content in terms of end-member gas phase contribution. The initial composition is represented by U1 day 170 (selected because it appears to have little impact of wax) and the CO_2-rich

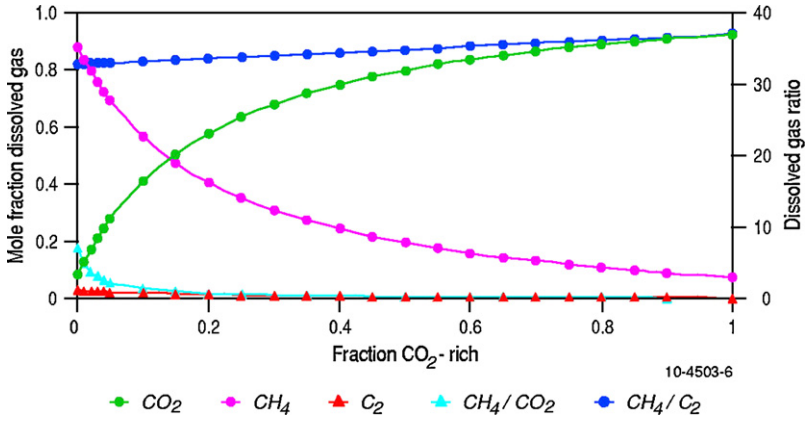

Fig. 10. Modelled composition of dissolved gas at U2 using a two end-member mixing model of CO_2-poor (in equilibrium with free gas with composition of U1 day 170) and CO_2-rich (in equilibrium with free gas with composition of U2 day 184). The fraction of CO_2-rich is plotted on the *X*-axis and on the *Y*-axis are plotted mol fraction of CO_2, CH_4 and C_2 (primary axis) and CH_4/CO_2 and CH_4/C_2 (secondary axis). *Note*: salinity at 0.006 mol% NaCl (Waarre Formation) is minimal on dissolved species. Note the solid lines are polynominal fit equations to the discrete data points.

end-member by U2 day 184. Gas phase fugacities were calculated using the Peng-Robinson EOS and the Henry's constants were applied to determine the dissolved gas species content going from 0 to 100% CO_2-rich (Fig. 10). It can be seen that the CO_2 content rises rapidly with >50% CO_2 occurring when only 15% of the CO_2-rich end-member is present. The data for U2 and U3 after breakthrough and prior to gas lift does not exceed ~50% CO_2 and the U3 data with CO_2 contents around 20–30% from day 150 to day 212 would only need 2–5% of the CO_2-rich end-member contribution to reach those values. This suggests that the sampled water had to be a mixture of water interacting with the CO_2-rich phase and water essentially at the initial reservoir conditions and only a very small proportion of the water sampled was from proximal to the gas–water contact. The configuration of the U-tube sampling system resulted in each water sample being a mixture of water sourced from the length of the perforated interval. The mixing ratios derived from the model indicate that additional constraints on flow modelling and geochemical modelling can be applied to understand the process of reservoir filling better.

One of the difficulties encountered during sampling was determining whether purely aqueous phase samples were collected or a mixture of aqueous phase and gas phase were drawn into the U-tube. The CO_2 content itself does not provide an effective measure, however, the relative solubilities of the hydrocarbons and the tracers result in significant differences between the exsolved and gas phase content. It is clear from the ratio data in Fig. 10 that the CH_4/C_2 data give a good indication when samples were purely exsolved ($CH_4/C_2 > 30$) and when gas phase was included in the sample ($CH_4/C_2 < 25$ Appendix 1). The SF_6 and Kr tracer model results also indicate only small increases are expected for the exsolved gas versus the contribution from a separate gas phase. Comparing the predicted exsolved composition with the data in Appendix 1 indicates that U2 was dominated by gas phase by day 163 and U3 by day 226 except for day 240 where the ratio of CH_4/C_2 and the tracer content suggest the gas sample was largely exsolved.

The carbon isotope data for CO_2 can also be used to determine the mass proportion (mixing ratio) of injected CO_2-rich gas that combines with the initial in-place CO_2-poor dissolved gas. For a two-component system ($\delta^{13}C\ CO_2$ initial gas for U1, U2 and U3 from Day 68 and $\delta^{13}C\ CO_2$ initial free gas = −6.7‰; average for Buttress-1 gas) with no isotope exchange the end-member contribution is given by:

$$\frac{X_{inj}}{X_{ini}} = \frac{\delta^{13}C^{m}_{CO_2} - \delta^{13}C^{ini}_{CO_2}}{\delta^{13}C^{inj}_{CO_2} - \delta^{13}C^{ini}_{CO_2}} \quad (3)$$

where X^{inj} = fraction of dissolved injected gas in total dissolved gas mixture, *inj* = injected (Buttress), *ini* = initial and *m* = measured.

The U2 and U3 mixing values (Table 2) using this overly simplified model are calculated based on the CO_2 gas content measured relative to the modelled gas content dissolved using a polynominal fit equation derived from discrete 'fraction CO_2-rich' increments as per Fig. 10. From Table 2 there is reasonable agreement (allowing for an experimental error of ±0.3‰ in measured values) between the fraction of injected CO_2 calculated using the two independent methods, supporting the concept of injected CO_2 initially arriving in a dissolved state. However, a more complete model is being developed involving isotopic fractionation of the CO_2 as it migrates and dissolves in the water along the migration path. Using a closed system Rayleigh model and setting the pH to 4, predicted by the reactive transport model (Kirste et al., 2009), a significant amount of the CO_2 (around 50%) dissolves but with only a small change in the isotopic composition of the injected CO_2 to around −6.2‰, instead of the −6.7‰ used in Table 2. However, fully development of this model awaits integration of the carbon isotopes with the $^{18}O/^{16}O$ data from free CO_2 and the associated formation waters.

4.3. Measures of breakthrough

Breakthrough, defined here as the first instance of the positive detection of added tracers (Fig. 9), is unequivocally supported by the results at U2 between sampling on day 100 (27th June 2008), which had no indication of allochthonous fluids, and day 121 (17th July 2008), by the simultaneous detection of an increase in mol% CO_2 and enrichment in $^{13}C\ CO_2$. The rapid rise in tracer content on day 163 (28th August 2008) lags by a further week the large positive offsets in the mol% CO_2 and $\delta^{13}C\ CO_2$ on day 156 (21st August 2008). This is likely due to the nature of the sample which according to the CH_4/C_2 ratio suggests it is largely but not entirely exsolved gas and the expected tracer content should increase by at least factor of 2–3. U1 shows a direct correlation between the rapid rise in CO_2 mol% and the tracer concentrations whereas a more complex relationship is seen at U3 that relates to the exsolved gas versus gas phase source components.

Reservoir simulation and flow modelling in the Waarre-C reservoir unit predicted breakthrough between 4 and 8 months after injection (Underschultz et al., 2011). The observed breakthrough in the Naylor Field is at the earlier end of the range forecast by dynamic modelling. Furthermore, the dynamic models did not

Table 2
Fraction of injected CO_2-rich dissolved gas derived from the carbon isotopic composition of CO_2 using a two end-member mixing model.

Day	U1	U2	U3	Fraction injected CO_2				
	‰	‰	‰	U1	U2 from Eq. (3)	U2 from mixing model#	U3 from Eq. (3)	U3 from mixing model#
68	−11.07	−12.73	−12.87	0	0		0	
86		−13.72	−13.07		−0.16	0	−0.03	0
101	−12.47	−12.98	−13.07	−0.32	−0.04	0	−0.03	0
121	−10.58	−10.90	−11.54	0.11	0.30	0.18	0.22	0.19
135		−10.85			0.31	0.20		
142	−10.72	−10.15		0.08	0.43	0.49		
156	−7.14	−7.19	−10.11	0.90	0.92	0.86	0.45	
163		−6.17	−9.00		1.09	0.88	0.63	0.69
170	−10.21	−6.65	−9.20	0.20	1.01	0.93	0.60	0.67
177	−9.66	−7.14	−8.31	0.32	0.93		0.74	0.71
184	−6.32	−6.20	−8.16	1.09	1.08		0.76	0.36
191	−9.02	−6.43	−8.56	0.47	1.04		0.70	0.62
198	−8.56	−6.34	−8.73	0.57	1.06		0.67	0.78
205	−9.83		−8.69	0.28			0.68	0.77
212	−8.08	−6.30	−8.46	0.68	1.07		0.71	0.72
219		−6.40	−7.56		1.05		0.86	
226	−9.46	−6.47	−5.97	0.37	1.04		1.12	0.84
233								
240	−7.89	−6.36	−8.72	0.73	1.06		0.67	0.76
248	−7.28	−6.19	−6.27	0.87	1.08		1.07	0.91
254	−6.97	−6.48	−6.26	0.94	1.04		1.07	
261	−6.59	−6.61		1.03	1.01			
268	−6.75	−6.49	−6.39	0.99	1.03		1.05	
275	−6.95	−7.43	−6.66	0.94	0.88		1.01	
279	−6.93	−6.92	−6.38	0.95	0.96		1.05	
293	−6.42	−5.88	−6.54	1.06	1.14		1.03	
303	−7.04	−6.28		0.92				

using an adjusted CO_2 free gas content of 0.008 mole fraction to match the initial dissolved CO_2 in U2 and U3.

have the resolution to predict these very small changes in CO_2 saturation and only considered breakthrough where the cell saturation increased by 20%. Therefore, the breakthrough event, as defined here, is not that significant in the context of our ability to model the system, which is largely governed by the free gas compositions during the transition to self-lift and thereafter.

4.4. Implications for Plume behaviour

Since the changes in CO_2 mol% and $\delta^{13}C$ CO_2 are relatively small at initial breakthrough, it signifies either the arrival of a dissolved CO_2 front or advance of the CO_2-rich fluid fingering down through regions of localised higher permeability and mixing with water during sampling, which provides a mix of fluids based on their relative mobility into the wellbore. The former mechanism is considered most likely as it is supported by modelling, which indicates a spatial resolution between an advanced dissolved CO_2 front and the main CO_2-rich supercritical fluid within the time–distance domain of the experiment (Underschultz et al., 2011). The general invariance in the wet gas content up to the time U2 (and U3) started transitioning to self lift is also consistent with the first arrival of a dissolved front. The large increase in CO_2 mol%, wet gas content and ^{13}C enrichment in gaseous CO_2 by day 156 (21st August 2008) signifies the intake at U2 accessing the main CO_2–CH_4 fluid front and the free gas contributing to the mix of fluids. Continual filling of the Naylor structure resulted in the downward movement of the GWC by 2.3 m (top of U2 inlet filter), resulting in U2 becoming solely self-lifting gas at surface on day 177 (11th September 2008).

The carbon isotopic composition of the indigenous gaseous CO_2 in the Naylor Field is depleted in ^{13}C by 4.5‰ compared to the injected gaseous CO_2 as would their dissolved $CO_{2(aq)}$ counterparts show a similar isotopic difference. Mixing of these different CO_2 sources leads to modest changes in $\delta^{13}C$ CO_2 and confirms the viability of this natural isotopic tracer in the Waarre-C sandstone reservoir. In the Weyburn project, more heavily depleted CO_2 ($\delta^{13}C$ approx. −20.4‰) was used. However, the carbonate-rich reservoir led to initial buffering of the isotopic shift with only small changes in ^{13}C DIC found as a result of carbonate mineral dissolution producing ^{13}C enriched isotopic signature and CO_2 dissolution producing a more ^{13}C depleted signature (Shevalier et al., 2004). Nevertheless, over a more extended period of 40 months of injection, the $\delta^{13}C$ of the CO_2 and HCO_3^- at the observation wells had decreased by 4.5 and 9.9‰, respectively (Raistrick et al., 2006). In the Frio Brine pilot experiment involving injection of ~1600 tonnes of very isotopically light CO_2 into a saline sandstone reservoir, mixing resulted in even more dramatic isotopic shifts of 30‰ (Kharaka et al., 2006). At the CO2CRC Otway Project, the observed carbon isotopic fractionation ($\Delta\delta^{13}C$) between the gaseous CO_2 (at U1) and DIC (at U2) of ~10.5‰ is slightly greater than the expected fractionation of ~8–9‰ at the surface temperature (pre-breakthrough: at U1 $\delta^{13}C$ CO_2(g) averages −11.0‰; CO_2(g) to HCO_3^- at pH 5.9 with isotopic fractionation (α) = 1.0085 @ 20 °C (Mook et al., 1974); U2 $\delta^{13}C$ DIC averages 0.55‰), suggesting a Rayleigh-type process may be taking place during the de-pressuring to collect the low pressure isotube gas sample. During de-pressuring of the holding cylinder the majority of the gas is released to atmosphere prior to collection of the low pressure isotube exsolved gas sample making such a process likely.

The maximum CO_2 content in U2 and U3 seen after gas lift is ~60 mol%, which is lower than the average 75.4 mol% CO_2 of the injected fluid. This most likely represents local mixing of the injected fluid with the methane-dominant residual gas in the pore space along the migration pathway and within the vicinity of the Naylor-1 wellbore. We conceptualize that the injected gas travels under strong buoyant forces until it reaches the gas cap. Within the gas cap the injected gas is denser than the methane, leading

to the injected gas spreading laterally and mixing with the native methane. At U1, the arrival of CO_2-rich fluid results in the CO_2 content being considerably lower at ~20 mol%. The Waarre-C reservoir is very heterogenous with high permeability regions interdispersed with zones of low permeable shaly baffles (Dance et al., 2009). Current reservoir models show CO_2-rich fluid in permeable zones within the residual gas cap between U1 and U2 at the wellbore. It is apparent from the U1 results that CO_2-rich fluid can be emplaced even higher up in the residual gas column under the right geological conditions. Given the limitation of only one observation borehole in a complex geologic system it is unlikely that a single plausible scenario can be identified. However, the bulk behaviour of the system is important because the compositions of the sampled gas inform any estimate for storage volume available within the Waarre-C reservoir (Underschultz et al., 2011).

The decrease in CO_2 from 55 to 60 mol% immediately after gas lift of U2 and U3 to an average around 48 mol% 11 months later is significant (Fig. 5). This is accompanied by a gradual increase of CO_2 from 20 mol% up to ~30 mol% in U1. These shifts in the CO_2 mol% for the three U-tubes may be partly in response to the gas cap moving towards equilibrium between the free gas and gas dissolved in the residual formation water. The existence of a horizontally continuous GWC is unlikely (Underschultz et al., 2011) due to the presence of many permeability baffles and porosity/permeability heterogeneity within the Waarre-C reservoir (Dance et al., 2009). As the gas cap expands, dynamic fluid flow modelling predicts the retention of an estimated 40–50% residual water in the pore space (Underschultz et al., 2011) and based on CO_2 core flooding experiments on sandstone from CRC-1). The attenuation to lower CO_2 content with time for U2 and U3 is likely to be due to the mixing of the initial CO_2-poor residual gas with the arriving CO_2-rich injected gas. Mass balance calculations of 20% residual methane gas with 1.5 mol% CO_2 and 30% injected gas with 75.4 mol% CO_2 (and 50% residual water) gives a final composition of 46 mol% CO_2; similar to the gas composition at U2 and U3 by mid-December 2009 (Fig. 5). On the other hand, the gradual increase of CO_2 mol% at U1 is likely a process of continual mixing between the CO_2-rich and CH_4-rich gases higher up into the gas column over a similar timeframe.

Dissolution will also be another mechanism for CO_2 attenuation. For 52 mol% CO_2 in the free gas, there is 92 mol% CO_2 in the dissolved gas at equilibrium; dissolution being a relatively rapid process (Shevalier et al., 2004). Since different volumes of residual water and gas occupy the available pore space, the amount of CO_2 that can be dissolved in the proximal residual water is relatively significant (~47 kg CO_2/tonne formation water (Zhenhao et al., 1992) (http://www.geochem-model.org/models.htm) and this will impact on the overall composition of the free gas, especially for U2 and U3. The effects of mixing and dissolution are competing processes and the quantitative contributions of each process are yet to be fully understood with respect to U-tube composition and tracer content. Continued sampling and analysis over the coming years should help resolve these issues.

5. Conclusions

The CO2CRC Otway Project is focussed around 3 wells, the Buttress-1 supply well, the CRC-1 injection well and the Naylor-1 observation well. Gas geochemistry of samples taken at the Naylor-1 observation well provides a direct measure of breakthrough of the mixed CO_2–CH_4 fluid injected at the CRC-1 well. This was achieved in the context of a depleted natural gas reservoir. Both the molecular and carbon isotopic compositions of CO_2 and tracers show positive responses at breakthrough; occurring between the samples taken 100–121 days after injection began and after the addition of 10,000–12,600 tonnes of mixed CO_2–CH_4 fluid. Since there is sufficient carbon isotopic differentiation between baseline and injected CO_2, both the chemical and carbon isotope data are useful in tracing the fate of the injected CO_2.

Following breakthrough, the CO_2 content rose to ~60 mol%, well below the 75.4 mol% CO_2 in the slightly modified Buttress-1 injected fluid. The difference is a result of mixing of the injected fluid with methane-rich/CO_2-poor residual gas (~20% methane-saturated formation water) encountered along the 300 m migration distance between the injection and observation wells and with the CH_4-rich/CO_2-poor residual gas column. The composition of the produced U-tube gases continues to evolve with time, even though the gas–water contact has moved below the lowest sample point. The CO_2 content in the upper U-tube (initially within the residual gas column) has gradually increased to ~30 mol%. On the other hand, the lower two U-tubes (initially below the GWC) show a gradual decrease from a maximum of 60 mol% in CO_2 to a current value averaging around 48 mol% CO_2, 21 months after injection began. The reduction in mol% CO_2 of the free gas phase is likely to be in response to partitioning between dissolved and free gas phases and the inefficient mixing of the residual CO_2-poor residual gas, the introduced CO_2-rich injected gas and the residual formation water, a re-distribution process occurring over a residence time of many months. This would also imply a less than optimum gas sweep of formation water as the GWC moves down with progressive filling of the Naylor structure. Hence, the storage capacity of supercritical CO_2 with the Naylor closure requires that we take into account both the dissolved and residual free CH_4 already in the system (Underschultz et al., 2011). Ignoring the impact of native free and dissolved CH_4 will lead us to an erroneously larger estimate of storage capacity.

The injection phase of the CO2CRC Otway Project which commenced on 18th March 2008 concluded on 28th August 2008 with the sequestration of 65,445 tonnes of mixed CO_2–CH_4 fluid, though sampling still continues. Breakthrough of the CO_2 at the observation well has been observed within the forecast time range of initial fluid flow and reservoir simulation models. The collection of physical fluids has been crucial in pinpointing breakthrough and high pressure sampling is found to be superior to low pressure samples under the current configuration for the U-tube collector. Given the restrictions imposed by the wellbore in the deployment of the trilevel U-tube assembly (e.g. use of a single packer), the responses of the U-tubes were relatively independent, although communication between the lower two U-tubes was evident when these were both sampling liquid or gas phases of similar composition.

Importantly, the CO2CRC Otway Project has demonstrated how to operate a geochemistry sampling system for M&V activities at a CO_2 storage site integrated with other essential M&V operations. The multilevel U-tubes have again proven to be robust over an extended timeframe and have provided geochemistry data that illuminates the processes by which injected CO_2-rich gas will fill a depleted gas reservoir. A multidisciplinary approach has been crucial in providing a wealth of complementary data that will allow calibration and refinements to fluid flow and reservoir simulation models and increased understanding of physical and chemical processes. Although in a research environment, the CO2CRC Otway Project has enabled us to better anticipate the challenges for rapid deployment of carbon storage in a commercial environment at much larger scales.

Acknowledgements

The authors would like to thank the significant contributions of a large interdisciplinary team working on the Otway Project. Particularly, the CO2CRC Otway Project manager Sandeep Sharma, geological and fluid flow modelling by Tess Dance, Josh Xu and

Lincoln Paterson, assurance monitoring by Allison Hortle, Ulrike Schacht, Patrice DeCaritat, Zoe Loh and David Etheridge and aqueous geochemistry by Ernie Perkins. The authors gratefully acknowledge the field sampling team of Kate Hill, Leon Meggs, Toby Kidd and Giorgio Palmeri from the Water Quality Laboratory at Deakin University (Warrnambool Campus), Ziqing Hong, Neel Jinadasa and Junhung Chen from the Isotope and Organic Geochemistry Laboratory, Geoscience Australia, Canberra for the molecular and carbon isotopic compositional results and SF_6 analysis, and Se Gong and Stephen Sestak from CSIRO Earth Science and Resource Engineering, Sydney for analysis of the tracers SF_6, Kr and CD_4.

Appendix A. Supplementary data

Supplementary data associated with this article can be found, in the online version, at doi:10.1016/j.ijggc.2011.03.011.

References

Bachu, S., Gunter, W.D., 2004. Acid–gas injection in the Alberta basin, Canada: a CO_2-storage experience. In: Baines, S.J., Worden, R.H. (Eds.), Geological Storage of Carbon Dioxide, vol. 233. Geological Society, London, Special Publications, pp. 225–234.

Boreham, C.J., Underschultz, J., Stalker, L., Freifeld, B., Volk, H., Perkins, E., 2007. Perdeuterated methane as a novel tracer in CO_2 geosequestration. In: Farrimond, P., et al. (Eds.), The 23rd International Meeting on Organic Geochemistry. Torquay, England, 9th–14th September 2007, Book of Abstracts, pp. 713–714.

Boreham, C.J., Edwards, D.S., 2008. Abundance and carbon isotopic composition of *neo*-pentane in Australian natural gases. Organic Geochemistry 39, 550–566.

Boreham, C.J., Chen, J., Hong, Z., 2008. Baseline study on sub-surface petroleum occurrences at the CO2CRC, Otway Project, western Victoria. In: PESA Eastern Australasian Basins Symposium III , Sydney, 14–17 September 2008, pp. 489–499.

Dance, T., Spencer, L., Xu, J.Q., 2009. Geological characterization of the Otway pilot site: what a difference a well makes. Energy Procedia 1, 2871–2878.

de Caritat, P., Kirste, D., Hortle, A., 2009. Composition and levels of groundwater in the CO2CRC Otway Project area, Victoria, Australia: establishing a pre-injection baseline. In: 24th International Applied Geochemistry Symposium , Fredericton, New Brunswick, Canada, 1–4 June 2009, Proceedings Volume 2, pp. 667–670.

Etheridge, D.M., Leuning, R., de Vries, D., Dodds, K., 2005. Atmospheric Monitoring and Verification Technologies for CO_2 Storage at Geosequestration Sites in Australia. CO2CRC Report; No. RPT05-0134. CO2CRC, Canberra, p. 81.

Fernandez-Prini, R., Alvarez, J.L., Harvey, A.H., 2003. Henry's constants and vapor–liquid distribution constants for gaseous solutes in H_2O and D_2O at high temperatures. Journal of Physical and Chemical Reference Data 32, 903–916.

Freifeld, B.M., Trautz, R.C., Yousif, K.K., Phelps, T.J., Myer, L.R., Hovorka, S.D., Collins, D., 2005. The U-tube: a novel system for acquiring borehole fluid samples from a deep geologic CO_2 sequestration experiment. Journal Geophysical Research 110, B10203, doi:10.1029/2005JB003735.

Freifeld, B.M., Trautz, R.C., 2006. Real-time quadrupole mass spectrometer analysis of gas in borehole fluid samples acquired using the U-tube sampling methodology. Geofluids 6, 217–224, doi:10.1111/j.1468-8123.2006.00138.x.

Freifeld, B.M., Perkins, E., Underschultz, J., Boreham, C., 2009. The U-tube sampling methodology and real-time analysis of geofluids. In: 24th International Applied Geochemistry Symposium , 1–4 June 2009, Fredericton, N.B., Canada.

Gale, J., 2004. Why do we need to consider geological storage of CO_2? In: Baines, S.J., Worden, R.H. (Eds.), Geological Storage of Carbon Dioxide, vol. 233. Geological Society, London, Special Publications, pp. 7–15.

Gunter, W.D., Bachu, S., Benson, S., 2004. The role of hydrogeological and geochemical trapping in sedimentary basins for secure geological storage of carbon dioxide. In: Baines, S.J., Worden, R.H. (Eds.), Geological Storage of Carbon Dioxide, vol. 233. Geological Society, London, Special Publications, pp. 129–145.

Helgeson, H.C., 1969. Thermodynamics of hydrothermal systems at elevated temperatures and pressures. American Journal of Science 267, 729–804.

Hennig, A., Etheridge, D., de Caritat, P., Watson, M., Leuning, R., Boreham, C., de Vries, D., Sherlock, D., Sharma, S., 2008. Assurance monitoring in the CO2CRC Otway Project to demonstrate geological storage of CO_2: review of the environmental monitoring systems and results prior to the injection of CO_2. Conference Proceedings (DVD), Extended Abstract. The APPEA Journal 48.

Hepple, R., Benson, S., 2003. Implications of surface leakage on the effectiveness of geologic storage of carbon dioxide as a climate change mitigation strategy. In: Gales, J., Kaya, Y. (Eds.), Proceedings of the 6th International Conference on Greenhouse Gas Control Technologies. Kyoto, Japan, September 30–October 4 2002. Pergamon, pp. 261–266.

Hovorka, S.D., Benson, S.M., Doughty, C., Freifeld, B.M., Sakurai, S., Daley, T.M., Kharaka, Y.K., Holtz, M.H., Trautz, R.C., Nance, H.S., Myer, L.R., Knauss, K.G., 2006. Measuring permanence of CO_2 storage in saline formations: the Frio experiment. Environmental Geosciences 13, 105–121.

Jaubert, J., Mutelet, F., 2004. VLE predictions with the Peng–Robinson equation of state and temperature dependent k_{ij} calculated through a group contribution method. Fluid Phase Equilibria 224, 285–304.

Jeirani, Z., Lashanizadegan, A., Ayatollahi, Sh., Javanmardi, J., 2007. The possibility of wax formation in gas fields: a case study. Journal of Natural Gas Chemistry 16, 293–300.

Kharaka, Y.K., Cole, D.R., Hovorka, S.D., Gunter, W.D., Knauss, K.G., Freifeld, B.M., 2006. Gas–water–rock interactions in Frio Formation following CO_2 injection: implications for the storage of greenhouse gases in sedimentary basins. Geology 34, 577–580.

Kirste, D., Perkins, E., Boreham, C., Freifeld, B., Stalker, L., Schacht, U., Underschultz, J., 2009. Geochemical modelling and formation water monitoring at the CO2CRC Otway Project, Victoria, Australia. In: 24th International Applied Geochemistry Symposium , 1–4 June 2009, Fredericton, N.B., Canada.

Krause Jr., D., Benson, B.B., 1989. The solubility and isotopic fractionation of gases in dilute aqueous solutions IIa – solubilities of the noble gases. Journal of Solution Chemistry 18, 823–873.

Leuning, R., Etheridge, D.M., Luhar, A.K., Dunse, B.L., 2008. Atmospheric monitoring and verification technologies for CO_2 geosequestration. International Journal of Greenhouse Gas Control 2, 401–414.

Majer, V., Sedlbauer, J., Bergin, G., 2008. Henry's law constant and related coefficients for aqueous hydrocarbons, CO_2 and H_2S over a wide range of temperature and pressure. Fluid Phase Equilibria 272, 65–74.

Mito, S., Xue, Z., Ohsumi, T., 2008. Case study of geochemical reactions at the Nagaoka CO_2 injection site, Japan. International Journal of Greenhouse Gas Control 2, 309–318.

Mook, W.G., Bommerson, J.C., Stavermen, W.H., 1974. Carbon isotope fractionation between dissolved bicarbonate and gaseous carbon dioxide. Earth and Planetary Science Letters 22, 169–176.

Peng, D.Y., Robinson, D.B., 1976. A new two-constant equation of state. Industrial and Engineering Chemistry Fundamentals 15, 59–64.

Peng, D.Y., Robinson, D.B., 1980. Two- and three-phase equilibrium calculations for coal gasification and related processes. Thermodynamics of aqueous systems in the industrial applications. ACS Symposium Series 393, 393–414.

Raistrick, M., Shevalier, M., Mayer, B., Durocher, K., Perez, R., Hutcheon, L., Perkins, E., Gunter, B., 2006. Using carbon isotope ratios and chemical data to trace the fate of injected CO_2 in a hydrocarbon reservoir at the IEA Weyburn Greenhouse Gas Monitoring and Storage Project, Saskatchewan, Canada. In: GHGT-8 , Trondheim, Norway, June 19–22, Extended Abstract.

Reid, R.C., Prausnitz, J.M., Sherwood, T.K., 1977. The Properties of Gases and Liquids, 3rd edition. McGraw-Hill, New York.

Ringrose, P., Atbi, M., Mason, D., Espinassous, M., Myhrer, Ø., Iding, M., Mathieson, A., Wright, I., 2009. Plume development around well KB-502 at the In Salah CO_2 storage site. First Break 27, 85–89.

Schilling, F., Borm, G., Würdemann, H., Möller, F., Kühn, M., CO2SINK Group, 2009. Status report on the first European on-shore CO_2 storage site at Ketzin (Germany). Energy Procedia 1 (February (1)), 2029–2035.

Sharma, S., Cook, P., Berly, T., Anderson, C., 2007. Australia's first geosequestration demonstration project – the CO2CRC Otway Basin Pilot Project. The APPEA Journal 47, 257–268.

Sharma, S., Cook, P., Berly, T., Lees, M., 2009. The CO2CRC Otway Project: overcoming challenges from planning to execution of Australia's first CCS project. Energy Procedia 1, 1965–1972.

Shevalier, M., Durocher, K., Perez, R., Hutcheon, I., Mayer, B., Perkins, E., Gunter, W., 2004. Geochemical monitoring of the gas–water–rock interaction at the IEA Weyburn CO_2 monitoring and storage project, Saskatchewan, Canada. In: Wilson, M., Morris, T., Gale, J., Thambimuthu, K. (Eds.), Proceedings of the 7th International Conference on Greenhouse Gas Control Technologies, vol. II, part 2. Elsevier, Amsterdam, pp. 2135–2139.

Søreide, I., Whitson, C.H., 1992. Peng-Robinson predictions for hydrocarbons, CO_2, N_2, and H_2S with pure water and NaCl brine. Fluid Phase Equilibria 77, 217–240.

Stalker, L., Boreham, C., Perkins, E., 2009. A review of tracers in monitoring CO_2 breakthrough: properties, uses, case studies, and novel tracers. In: Grobe, M., Pashin, J.C., Dodge, R.L. (Eds.), Carbon Dioxide Sequestration in Geological Media – State of the Science. AAPG Studies in Geology 59, 595–608.

Trew, M., O'Sullivan, M.J., Yasuda, Y., 2001. Modeling the phase partitioning behavior of gas tracers under geothermal reservoir conditions. Geothermics 30, 655–695.

Underschultz, J., Freifeld, B., Boreham, C., Stalker, L., Schacht, U., Perkins, E., Kirste, D., Sharma, S., 2008. Geochemistry monitoring of CO_2 storage at the CO2CRC Otway Project, Victoria. Conference Proceedings (DVD), Extended Abstract. The APPEA Journal 48.

Underschultz, J., Boreham, C., Stalker, L., Freifeld, B., Xu, J., Kirste, D., Dance, T., 2011. Geochemical and hydrogeological monitoring and verification of carbon storage in a depleted gas reservoir: examples from the Otway Project, Australia. International Journal of Greenhouse Gas Control, doi:10.1016/j.ijggc.2011.02.009.

Vandeweijer, V.P., van der Meer, L.G.H., Hofstee, C., Hoore, D.D., Mulders, K., 2009. CO_2 storage and enhanced gas recovery at K12-B. In: 71st EAGE Conference & Exhibition , Amsterdam, The Netherlands, 8–11 June 2009.

Vitu, S., Privat, R., Jaubert, J., Mutelet, F., 2008. Predicting the phase equilibria of CO_2 + hydrocarbon systems with the PPR78 model (PR EOS and k_{ij} calculated through a group contribution method). The Journal of Supercritical Fluids 45, 1–26.

Vogel, J.C., Grootes, P.M., Mook, W.G., 1970. Isotopic fractionation between gaseous and dissolved carbon dioxide. Zeitschrift fur Physik 230, 225–238.

Watson, M.N., Boreham, C.J., Rogers, C., 2006. Soil Gas Baseline Characterisation Study – Winter 2005 Survey. Otway Basin Pilot Project. CO2CRC Report No. PT06-0181.

White, D.J., Hirsche, K., Davis, T., Hutcheon, I., Adair, R., Burrowes, S., Graham, S., Bencini, R., Majer, E., Maxwell, S., 2004. Prediction, monitoring and verification of CO_2 movements. In: Wilson, M., Monea, M. (Eds.), IEA GHG Weyburn CO_2 Monitoring & Storage Project Summary Report 2000–2004. Proceedings of the 7th International Conference on Greenhouse Gas Control Technologies. September 5–9, 2004, Vancouver, Canada, pp. 73–148.

Zhenhao, D., Nancy, M., Weare, J., 1992. An equation of state for CH_4, CO_2 and H_2O II, mixtures from 0 to 1000 °C and from 0 to 1000 bar. Geochimica et Cosmochimica Acta 56, 2619–2631.

Zweigel, P., Arts, R., Lothe, A.E., Lindeberg, E.B.G., 2004. Reservoir geology of the Utsira Formation at the first industrial scale underground CO_2 storage site (Sleipner area, North Sea). In: Baines, S.J., Worden, R.H. (Eds.), Geological Storage of Carbon Dioxide, vol. 233. Geological Society, London, Special Publications, pp. 165–180.